JOURNAL OF GEOPHYSICAL RESEARCH, VOL. 106, NO. D16, PAGES 18,439–18,460, AUGUST 27, 2001

A hemispheric dust storm affecting the Atlantic and Mediterranean in April 1994: Analyses, modeling, ground-based measurements and satellite observations

Emin Özsoy and Nilgün Kubilay

Institute of Marine Sciences, Middle East Technical University, Erdemli, İçel, Turkey

Slobodan Nickovic

Euro-Mediterranean Centre on Insular Coastal Dynamics, Valletta, Malta

Cyril Moulin

Laboratoire des Sciences du Climat et de l'Environnement (CEA/CNRS), Gif-sur-Yvette, France

Abstract. One of the largest recorded dust tranpsort events originating from the great Sahara desert during April 1994 affected the entire region extending from the Caribbean to the Eurasian continent. This hemispherical transport of airborne dust took place during a series of storms that developed during the first three weeks of April in a background of low-index circulation. These repeated events are studied through the combined analyses and interpretation of atmospheric data, ground-based aerosol measurements, visibility observations, AVHRR and Meteosat visible band satellite data, and the results of Eta model simulations, including an aerosol transport component. The observations produce a consistent picture of the temporal and spatial development of the dust events, whose main features are used in parts to verify the model results. The rate of dust suspension from some areas of the western Sahara desert exceeded 1.5 mg m^{-2} h^{-1} and the maximum column integrated dust load reached 2 g m^{-2} during April 3-5 1994, when the first major suspension event produced two simultaneous pulses of dust moving in opposite directions across the subtropical Atlantic Ocean and the eastern Mediterranean Sea. These dust suspensions were created by surface winds resulting from subsidence on the northeastern side of a blocking anticyclone in the Atlantic region and subsequent winds of an intense developing cyclone in the Mediterranean-African region. In the following period, maximum dust loads of 4.5 and 2.5 g m^{-2} occurred on April 12 and 17, respectively, when new cyclones transported dust across the Mediterranean from Africa to Europe. The generation of the two dust pulses during the first even and the recurrent cyclone transport in the following period is shown to be the result of a large-scale, anomalous atmospheric circulation connected with blocking in the Atlantic Ocean and the interactions of upper air jets downstream of the blocking. The particular state of the hemispheric circulation during the studied period corresponded to the positive phase of the North Atlantic Oscillation (NAO). While previous statistical evidence has consistently linked dust transport in the region with the NAO signatures, we show the same connection on the basis of this case study.

1. Introduction

The aeolian transport of desert dust is an important modifier of climate, through its effects on the following: backscattering and absorption of solar and terrestrial radiation [*Miller and Tegen*, 1998, 1999; *Tegen et al.*, 1996], the heat budgets of the lower troposphere [*Alpert et al.*, 1998] and the surface layers of the ocean [*Schollaert and Merrill*, 1998], especially in the case of semienclosed seas [*Gilman and Garrett*, 1994], greenhouse gases [*Dentener et al.*, 1996], and marine biogeochemistry [*Duce et al.*, 1991; *Guerzoni et al.*, 1999].

Paper number 2000JD900796.
0148-0227/01/2000JD900796$09.00

The availability and abundance of desert dust in the atmosphere is directly affected by changes in climate [*Tegen et al.,* 1996], and there are indications that the dust events in the Mediterranean region have been increasing in the 1990s [*Avila and Peñuelas,* 1999]. Large-scale controls are anticipated. The North Atlantic Oscillation (NAO) is well correlated with Saharan dust events [*Moulin et al.,* 1997]. Saharan dust at Barbados Islands is found to depend on drought conditions and El Niño/Southern Oscillation (ENSO) [*Prospero and Nees,* 1986]. Large-scale controls are important in the eastern Mediterranean-Eurasian region, where the coupled land-ocean-atmosphere variability of the various regional seas, and the atmosphere appears to have a synchronized response to these controls [*Özsoy et al.,* 1999].

Transport of dust from the great Sahara into the Mediterranean Sea and the Atlantic Ocean tends to occur simultaneously under exceptional cases [*Moulin et al.,* 1997]. For the studied case of April 1994, maximum dust concentrations for the last 30 years were measured at Barbados [*Li et al.,* 1996; *Andreae,* 1996], and for the period 1983-1994 at Sal Island [*Moulin,* 1997], which possibly corresponded to one of the largest of such events in the eastern Mediterranean, where the record is relatively shorter. The authors experienced the event in Erdemli, on the Mediterranean coast of Turkey, where the screening of the solar radiation produced a marked decrease in visibility and partial darkness during daytime. The maximum measured dust concentration at this site was 1.6 mg/m^3.

Despite their great importance, the typical meteorological conditions leading to dust suspension and transport are difficult to predict or have not been sufficiently well characterized, because they seem to depend on the specific conditions of each region.

Dust is mobilized from the Sahara desert by aeolian processes and transported to the Atlantic Ocean, Mediterranean-European and Indian Ocean regions [e.g., *Husar et al.,* 1997]. The mobilization of dust has seasonal as well as diurnal cycles that depend on source characteristics as well as wind climatology. Results derived from satellite observations [*Husar et al.,* 1997], surface visibility data [*Mbourou et al.,* 1997], and the fusion of the various sources of data [*Husar and Husar,* 1998] show a seasonal shift in the westward plume of aerosols from the Sahel or sub-Saharan region in winter and spring to the central Saharan region at a more northerly latitude in summer. There has been some controversy assigning to either the Sahel region or the Saharan region more weight as the main source region of African dust [e.g., *Mbourou et al.,* 1997], but finally it seems clear that the anthropogenically disturbed soils of the Sahel region also have a significant contribution in addition to the Saharan sources. In summer the transported aerosols are almost twice as large as in winter [*Husar et al.,* 1997]. The increased numbers of tropical storms and wave disturbances within the tropical easterly jet transport dust from Africa toward the tropical Atlantic, reaching the Caribbean Sea and North America [*Prospero,* 1981, 1999; *Karyampudi and Carlson,* 1988; *Ott et al.,* 1991, *Perry et al.,*, 1997].

Some Mediterranean dust events have been connected with North African "Sharav" cyclones [*Alpert and Ziv,* 1989] typically occurring in the winter and spring, and emerging into the eastern Mediterranean from south of the Atlas Mountains [*Reiter,* 1979; *Brody and Nestor,* 1980]. *Egger et al.* [1995] have suggested an increase in baroclinicity near the coast as a result of the approach of the polar front in spring, having a major impact on the formation of Sharav cyclones, successfully incorporated into a dynamical model.

In winter and spring the Mediterranean Sea is affected by two upper air jet streams: the polar front jet stream (PFJ), originally located over Europe, meanders and affects the Mediterranean region during periods of low-index circulation, while the subtropical jet stream (STJ) is typically located over northern Africa. The combined effects of these westerly jets in winter and spring support easterly propagating extratropical cyclone systems as well as frequent cyclogenesis in the Mediterranean-African region [*Reiter,* 1975]. One of the important Mediterranean cyclogenesis mechanisms, first suggested by *Reiter* [1975], later confirmed by *Prezerakos et al.* [1990] and *Prezerakos* [1998] is the interactions of the polar front jet stream (PFJ) and the subtropical jet stream (STJ).

Alpert and Ziv [1989] and *Alpert and Ganor* [1993] demonstrated a strong relationship between the jet stream and the cyclogenesis over north Africa, resulting in the dust plume intrusion in the Mediterranean. A relationship between the jet streams and severe dust storms has also been recognized by *Danielsen* [1974] in the case of the American continent and by *El-Tantawy* [1961] in the the case of the Middle East, who have suggested that the activity of the cyclones leading to dust transport were strongly correlated with the STJ and, in severe weather events, with the southward transition of the PFJ

We study the spectacular dust storm of April 1994 through analyses of ground- and satellite-based observations and model simulations. In section 2 we provide details of the data and methodology used, then in section 3 we interpret and discuss our results. Section 4 gives brief conclusions and suggestions for further research.

2. Methodology

2.1. Ground-Based Measurements

Aerosol measurements were available at Erdemli on the Turkish Mediterranean coast (36°N, 34°E; height, 21 m) [*Kubilay and Saydam,* 1995] and at island stations in the tropical Atlantic (Barbados, 13°N, 59°W), [*Li et al.*, 1996] and Sal Island (16.7°N, 23.0°W; height 125 m) [*Chiapello et al.,* 1995, 1997]. In the present study, dust concentration is computed from aluminum,

obtained by elemental analysis at Erdemli, and from silicon concentration at Sal Island.

Horizontal extinction coefficient calculated from standard (WMO) visibility measurements at meteorological stations were obtained from the Center for Air Pollution and Trend Analysis, Washington University (J. Husar, personal communication, 1999). Rawinsonde data were acquired from the National Climatic Data Center (NCDC) of the National Oceanic and Atmospheric Administration (NOAA).

2.2. Satellite Data

Both the AVHRR visible and infrared data from NOAA satellites and the Meteosat satellite were analyzed and used for comparisons. The daily composite images in Plate 1 were made by combining aerosol optical depth (AOD) for dust over the ocean, obtained from the VIS band of the Meteosat (following *Dulac et al.* [1992] and *Moulin* [1997], and infrared difference dust index (IDDI) over the continent obtained from its IR band (following a simplified version of the method by M. Legrand). Cloud pixels were then superimposed, as seen using the IR band, with a white color denoting the high-altitude and grey denoting the low-altitude clouds, to visualize weather systems responsible for the suspension and transport processes.

2.3. Atmospheric Model

The Eta regional atmospheric model, originally developed by the University of Belgrade and the Federal Hydrometeorological Institute of Yugoslavia, with further improvements made by the National Centers for Environmental Prediction, Washington, D. C. is used for the simulation of the atmospheric dynamics and dust transport. The model makes use of the numerical techniques and parameterizations, as discussed by *Janjic* [1977], [1984], *Mesinger et al.* [1988], and *Janjic* [1990, 1994]. The dynamics of the model is based on large-scale numerical solutions controlled by conservation of integral properties, energetically consistent time-difference splitting and the step-like mountain representation. The model physics consists of the viscous sublayer models over water, a turbulence closure scheme based on Kolmogorov-Heisenberg theory, the Betts-Miller-Janjic deep and shallow moist convection scheme, the land surface scheme, the grid-scale precipitation scheme, and the radiation scheme.

At this level of model development there are several simplifications introduced in our model setup. First, we assume that dust particles have a uniform size with a diameter of 2 μm, simplifying the real-particle size distribution. The chosen diameter falls into the interval of dust particles observed to travel longer distances [*Perry et al.*, 1997] and is well detected by satellite observations. Furthermore, dust concentration is also considered to be chemically passive and a substance that does not affect the atmospheric radiation processes. The radiation effects will be a matter of separate future development, assuming that they cannot significantly modify temperature profiles in our rather short-term model experiments.

The conservation equation for dust is integrated on line, within the Eta atmospheric model. The dust part of the model describes all the major components of the atmospheric dust cycle. Numerical schemes for advection, turbulent mixing in the free atmosphere, and horizontal diffusion of dust are analogous to the schemes used for other scalar variables in the model. Because the detailed description of the model is given elsewhere [*Nickovic and Dobricic,* 1996], and successfully tested in other cases [*Kubilay et al.*, 2000, *Nickovic et al.*, 1997], it is not repeated here. Further development of the model with other applications can be found in the work of *Nickovic et al.* [this issue].

The surface dust source points in the model are specified according to the *Wilson and Henderson-Sellers* [1984] global 1° x 1° vegetation data set. Vegetation types 70 (sand desert and barren land) and 71 scrub desert and semidesert) are used to define the dust source points in the model. Dust suspension from the Earth's surface is a function of the availability at the surface, soil wetness, and the applied wind stress (friction velocity) [*Nickovic and Dobricic,* 1996].

In designing the dust production scheme, the viscous sublayer model is used [*Nickovic et al.*, 1997], exploiting the physical similarity between turbulent mixing over the sea and over deserts [*Chamberlain,* 1986; *Segal,* 1990]. Following the analogy with momentum-heat-moisture-surface interchange of the atmospheric parameters, it is assumed that in the case of dust mixing a thin viscous sublayer just above the desert surface sublayer is created under smooth flow conditions. The transition toward the rough flow is happening with the increased turbulent mixing. Under fully developed turbulence the viscous sublayer vanishes and mobilization and saltation of particles over dust surfaces starts. Under such conditions there is an efficient interchange of dust material between the desert surface and the atmosphere. Ground wetness effects on dust production are incorporated as well. Once injected into the atmosphere, dust is transferred in the vertical by the vertical advection and vertical turbulent mixing processes. The vertical advection scheme conserves the dust mass and does not produce new maxima. Wet deposition due to precipitation is represented by a scavenging parameterization scheme. The dry deposition scheme takes into account gravitation settling effects.

The present model of dust suspension, transport, and deposition has produced reliable results in a number of earlier tests, where the concentration and spatial coverage of dust over the sea have been verified with satellite and ground-based dust measurements in the western and eastern basins of the Mediterranean for a number of major dust storms [*Nickovic and Dobricic,* 1996; *Kubilay et al.*, 2000; *Nickovic et al.*, this issue].

The April 1994 dust transport episode was simulated with the model domain covering most of the Sahara and

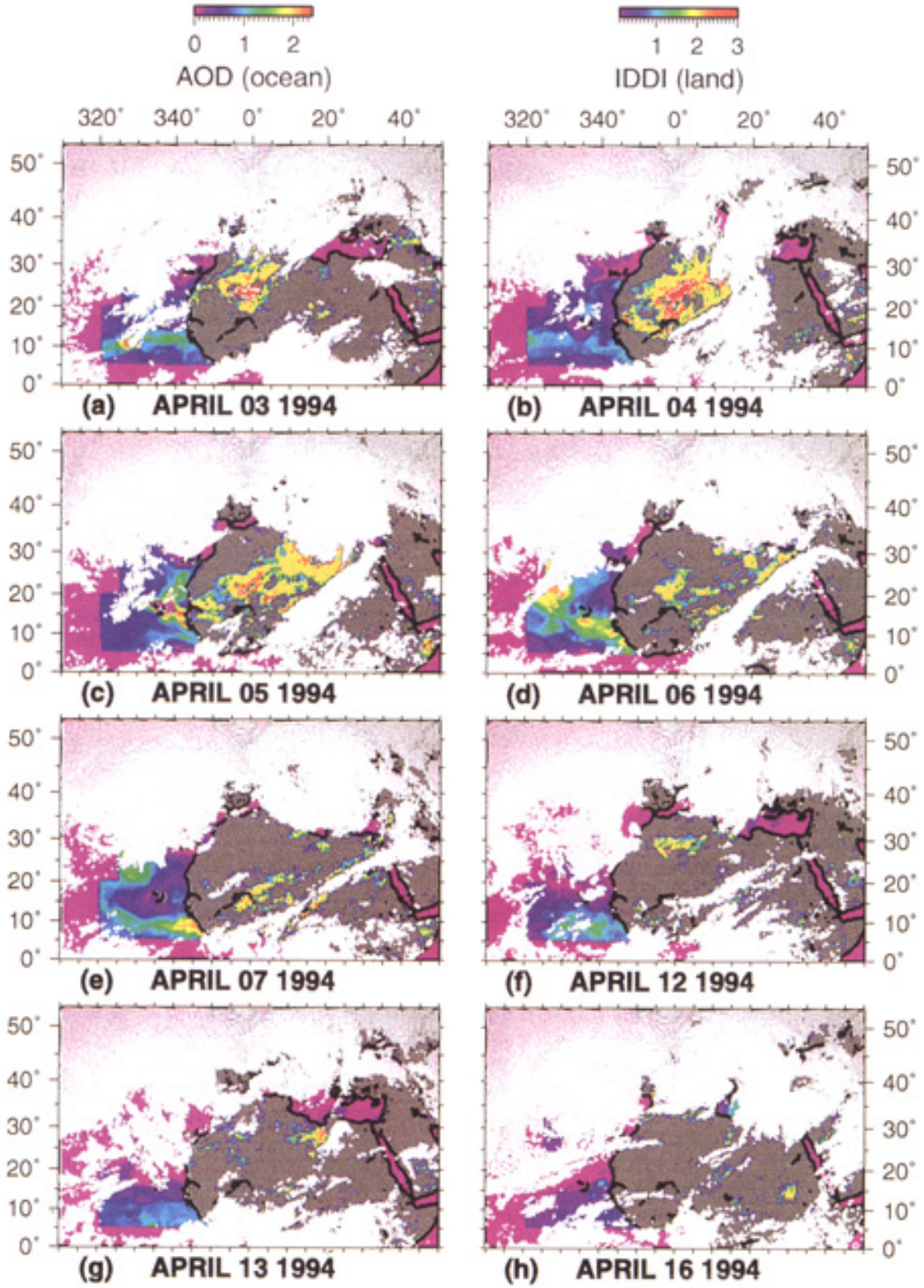

Plate 1. Satellite-derived daily composite images of aerosol optical depth (AOD) derived from Meteosat visible data over the sea and infrared difference dust index (IDDI) derived from raw counts of infrared data over land on (a) April 3, (b) April 4, (c) April 5, (d) April 6, (e) April 7, (f) April 12, (g) April 13, (h) April 16, 1994.

the Atlantic, with a resolution of 0.75° × 0.75° (horizontal) and 32 model vertical layers (distributed as 4 levels within the first 250 m, 7 levels within 0.25-1.00 km, 10 levels within 1-5 km and 11 levels within 5-10 km elevations). The model was run from March 28 to April 22, 1994, in a sequence of 24 hour simulations. The meteorological part of the model was initialized using the objective analyses of the European Center for Medium-Range Forecasts (ECMWF) with updates every 24 hours. The ECMWF fields were also used in order to specify the model lateral boundary conditions with updates every 6 hours. The model dust fields were updated every 24 hours, based on the previous day's run. The model topography and soil types, used to characterize desert areas, are shown in Figure 1.

3. Results and Discussion

3.1. Atmospheric Blocking and Jet Interactions

We first describe changes in the hemispherical weather in this section to identify the underlying features of the

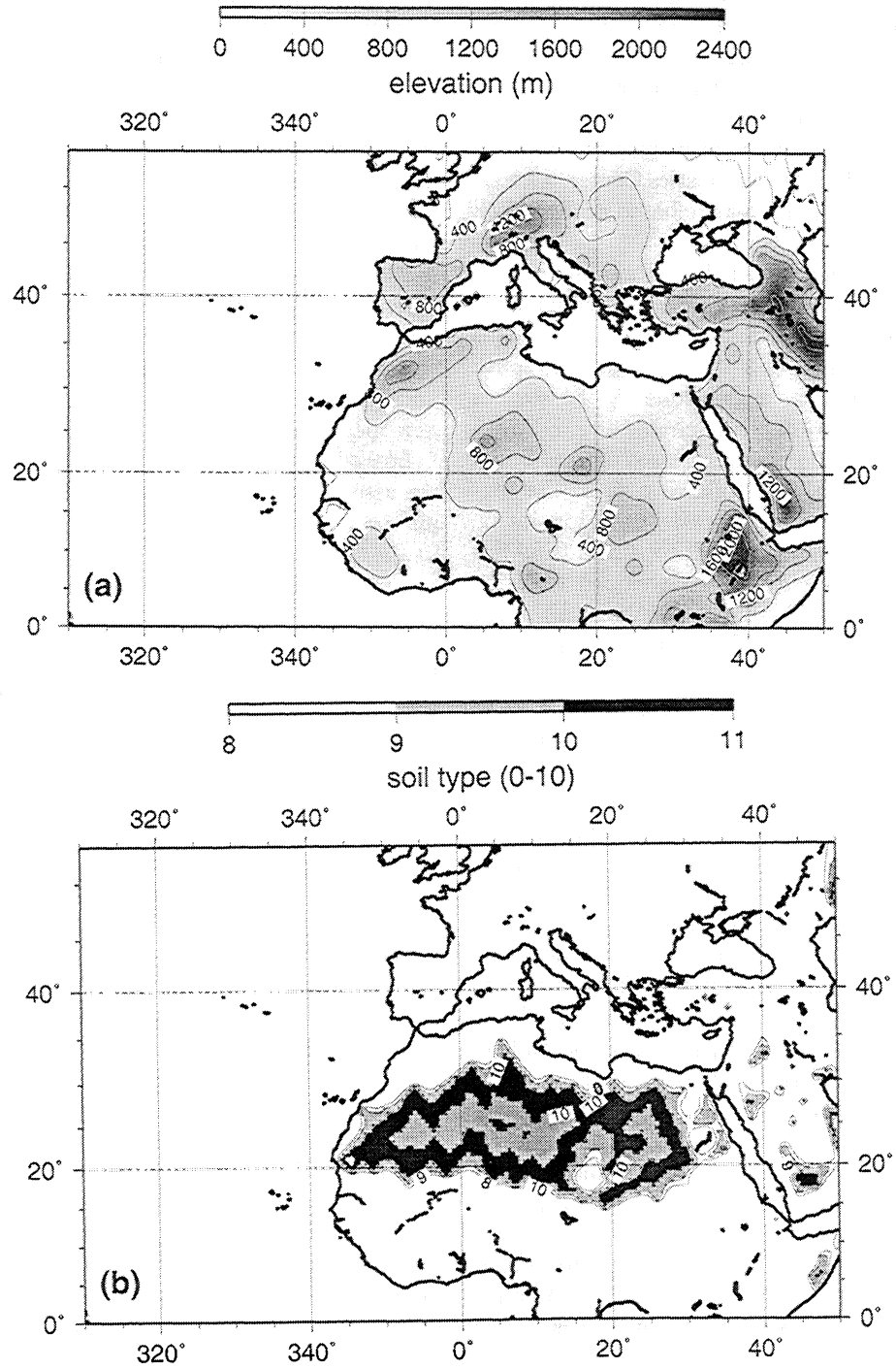

Figure 1. (a) Surface topography, and (b) soil-type classification showing desert and semidesert areas used in the model.

circulation and wind systems driving peak dust suspension and transport during the period of investigation.

The synoptic situation on April 1, 1994, was characterized by the subtropical high pressure at 35°N, 35°W, the subpolar (Icelandic) low pressure at 65°N, 10°W, both centered in the Atlantic Ocean, and the equatorial low pressure across the tropical Atlantic and the African continent. The Siberian high pressure dominated the Eurasian continent, except near the Middle East, where a cyclone had passed in the earlier period. The central Mediterranean was dominated by high pressure.

During the following period in the first part of April 1994 the hemispheric circulation undergoes an "index cycle," developing low zonal index (meridional) patterns and repeated cyclone activity that persists for more than 2 weeks. In Figures 2 and 3 we show the hemispheric development based on atmospheric data obtained from NOAA Climate Diagnostics Center, whereas the model results displayed later are based on ECMWF data initializations.

The geopotential height field at 500 hPa pressure level on April 1 (Figure 2a) shows a coherent zonal flow, excluding a dipole in the Atlantic Ocean (25°N). This dipole at midtroposphere is slightly shifted to the south relative to the subtropical anticyclone at the surface (not shown). An inspection of the circulation indicates that the subtropical high pressure pressed toward Spain around April 2-4, and in the following days, the uniform zonal jet at 500 hPa developed into a low-index, meridionally perturbed flow over Europe and the Middle East. On April 4 a cutoff low developed near the eastern part of the Atlas Mountains (35°N 10°E) in the western Mediterranean Sea. On April 5 (Figure 2b) the cutoff low, marking a deep cyclone, shifted east to about 35°N, 18°E on the 500 hPa geopotential field. The cyclone on the sea level pressure maps (not shown) later moved north to the Balkans and eastern Europe through the Gulf of Sirte, reaching the positions 42°N, 20°E on April 6; 52°N, 22°E on April 7; 60°N, 22°E on April 8; and disappearing thereafter. On April 9 (Figure 2c) the meandering of the zonal jet increases and extends from Europe across Asia into the Pacific region. On April 13 (Figure 2d) the low-index flow develops further and extends eastward from the mid-Atlantic region, with a weak jet shifted north of Europe. A cyclone persists over southern Europe and its surface center shifts to western North Africa on April 15, and moves once again over the Mediterranean on April 16. On April 17 the cyclone is evident in the 500 hPa geopotential height (Figure 2e) and affects north Africa till April 20. During the entire period of investigation the recurrent cyclone centers follow circular trajectories: after approaching the eastern Mediterranean from the west, they turn north and later west to be reformed in northwest Europe before moving east. The recurrent cyclones thus form a semistationary weather pattern in which the cyclones are diverted north before they are advected east, partially in agreement with the weakened jet flow over Europe observed in the 500 hPa geopotential fields.

The blocking circulation in the Atlantic region displayed in Figures 2 and 3, evidently having a prominent barotropic component, forces the upper tropospheric jet stream downstream of it to approach each other and come into contact in the following period. This is best displayed by a sequence of daily upper air winds in Figure 3. The shaded areas are the projections of the regions where the upper air speed exceeds 30 m/s, i.e., the cores of the polar and subtropical jet streams. During the later part of March and on April 1 (Figure 3a), there are two separate jet streams over the Atlantic and European regions, one located at high latitudes and the other at low latitudes; then on April 2 - 4, the two jets start to interact. On April 5 the zonal jet starts to get deformed and flows toward Africa, while meanders develop near its extension zone over Europe and the Middle East (Figure 3b). During April 5-7 the meridional pattern of circulation is further deformed, and the two jets, which come into contact in the preceding days, finally coalesce on April 9 (Figure 3c) to form a single jet extending from the Mediterranean-European region to central Asia near the Himalaya Mountains. By April 13 (Figure 3d) the subtropical jet becomes more coherent and strong compared to the polar jet, which develops new meanders but with smaller speed.

Low zonal index circulations in the atmosphere are often associated with "blocking," when a quasi-stationary air mass blocks and diverts the mean flow, as shown in the April 1994 case. Blocking typically develops in the midlatitudes, where it is normally least expected (based on destabilizing effects of zonal jets and baroclinicity) and accounts for a considerable portion of the low-frequency variability in the atmosphere [*Wallace and Blackmon*, 1983]. Modons, or coherent dipole vortices, arising through nonlinear processes, represent stable patterns (with a high pressure center located north of a low) embedded in a zonal mean flow which ideally develop blocking conditions [*McWilliams*, 1980; *Flierl et al.*, 1980]. We observe all of the above to be dominating the investigated case.

3.2. Dust Suspension and Transport

A review of satellite-derived daily composite images of dust-related AOD over the sea and IDDI over land, for the period of interest (Plate 1), shows the sources and distribution of consecutive dust events in the Mediterranean and subtropical Atlantic regions through the period. Corresponding to an increased momentum transport from the atmosphere toward the ground over the desert areas of Saharan Africa during either subsidence coming from the North Atlantic or cyclonic development in the Mediterranean-African regions, the IDDI shows an increased source activity (suspension) in the regions. In Plate 1, immediately after the period of increased IDDI over land, increased amounts of dust in the adjoining Atlantic Ocean and eastern Mediter-

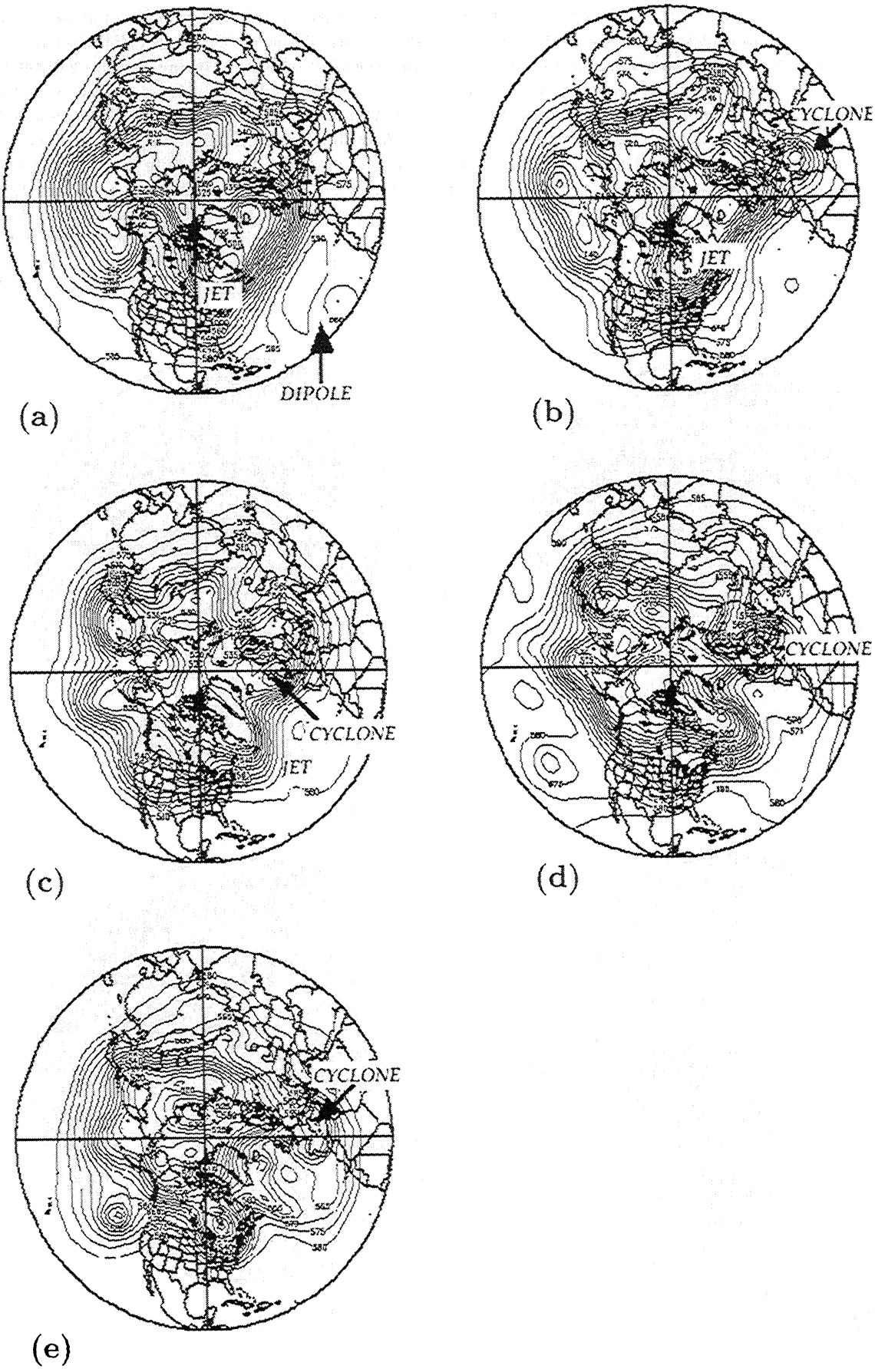

Figure 2. Geopotential height at 500 hPa pressure level for the Northern Hemisphere on (a) April 1, (b) April 5, (c) April 9, (d) April 13, (e) April 17. The source for the data is NOAA Climate Diagnostic Center (plotting page URL http://www.cdc.noaa.gov/HistData/).

ranean regions are evident from AOD measured over the ocean, confirming that the dust suspended over the Sahara is transferred to the adjoining ocean regions.

On April 3 and 4 (Plates 1a, 1b) we find a large area of suspended dust (IDDI) in the western great Sahara in agreement with the increased fluxes there (compare Figure 4a), which then moves east across the desert toward the Gulf of Sirte during the following days. On April 5 and 6 (Plates 1c, 1d), along with a decrease in the activity of the source areas in western Sahara (IDDI), new source areas of dust are formed in the east (compare Figures 4b, 4c). The dust cloud in the eastern Mediterranean (IDDI and AOD) is partially masked by the clouds of the developing cyclone between Tunisia and the Gulf of Sirte. During the same dates the dust cloud in western Sahara moves to the Atlantic where the AOD is increased to reach a peak near Sal Island on April 5 (Plate 1c), verified by ground measurements and model results later (Figure 10). During the initial phase of development on April 3-6 (Plates 1a-1d) the spreading of the dust into the subtropical Atlantic is observed to be in the form of a semicircular arc, suggesting a frontal structure of the dust storm extending into the ocean. On April 6 and 7 (Plate 1d,e), the dust

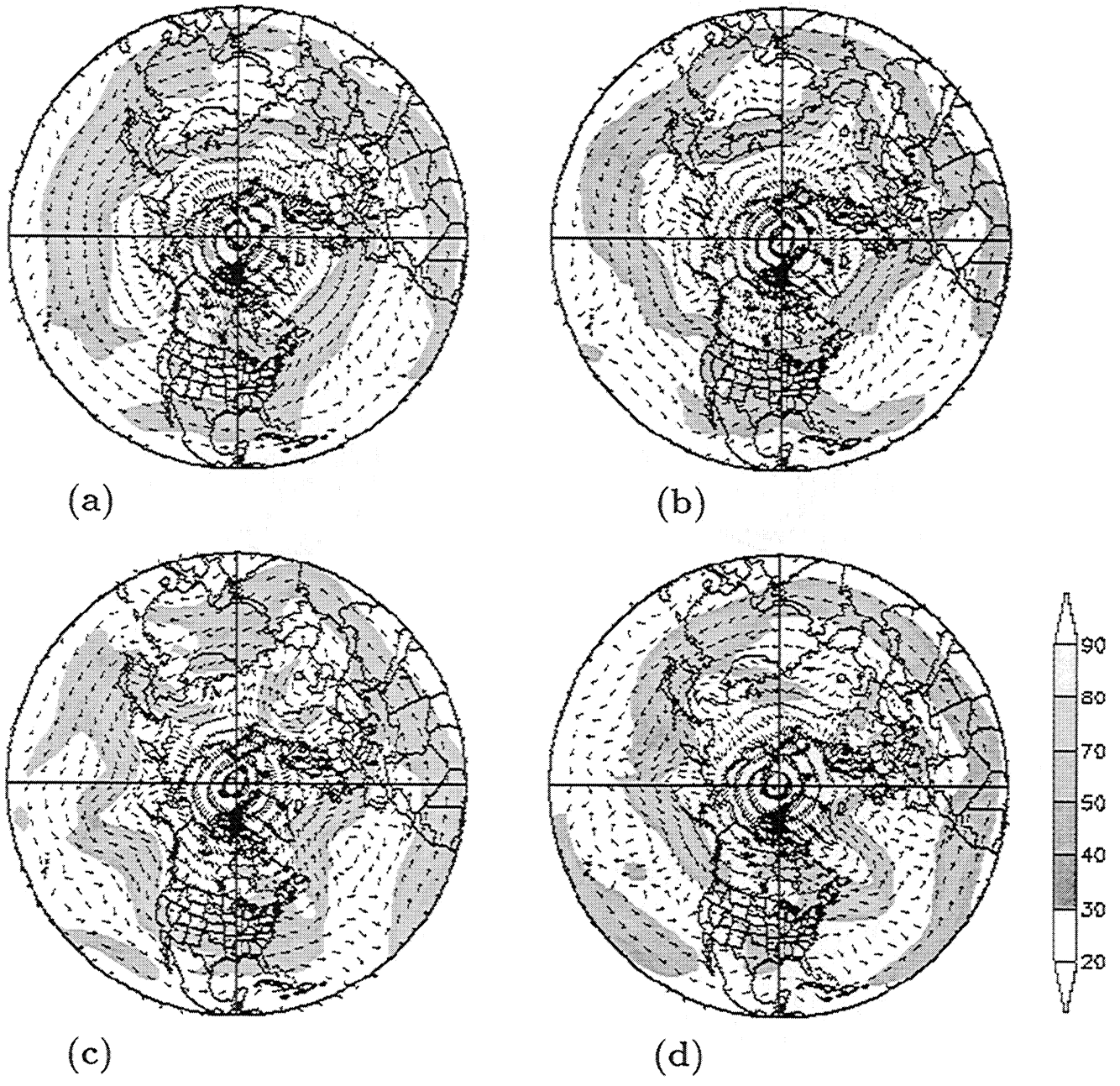

Figure 3. Daily wind speed (shading) and direction (unit vectors) at 250 hPa pressure level for the Northern Hemisphere on (a) April 1, (c) April 5, (c) April 9, (d) April 13, 1994. The source for the data is NOAA Climate Diagnostic Center (plotting page URL http://www.cdc.noaa.gov/HistData/).

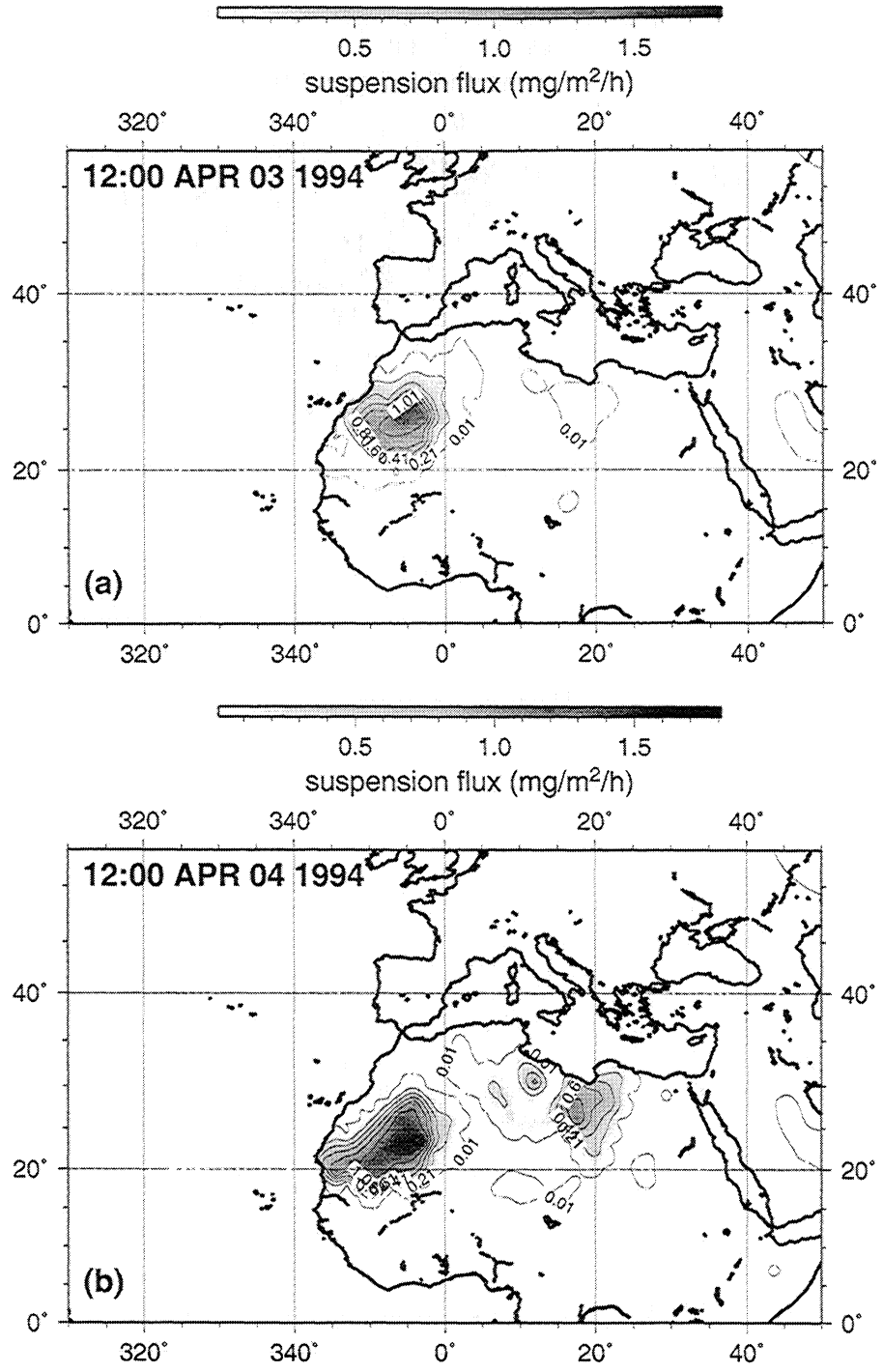

Figure 4. Model-generated dust suspension flux (mg $m^{-2}h^{-1}$) at 1200 UTC on (a) April 3, (b) April 4, (5) April 5, 1994.

front has reached the central part of the Atlantic Ocean, while the northern edge of the semi-circular front has been detached from the northwestern coast of Africa. We believe this detachment could be a result of the shallow layer of marine air arriving from the north along the northwest coast of Africa [*Tucker and Barry,* 1984] and intruding below the dust-laden air that originated from the Sahara.

On April 12-13 (Plates 1f, 1g) the warm front of a cyclone located over southern Europe sweeps over the region south of the Gulf of Sirte and transports dust to the central and eastern Mediterranean, while the transport to the subtropical Atlantic from the earlier, western Sahara source region appears to have been significantly reduced in comparison to early April. On the other hand, a continuous stream of dust from the sub-Saharan (Sahel) region of Africa appears to be transported to the Atlantic region throughout the studied month of April. This relatively steady pattern of transport could be related to the anthropogenic sources in the Sahel region

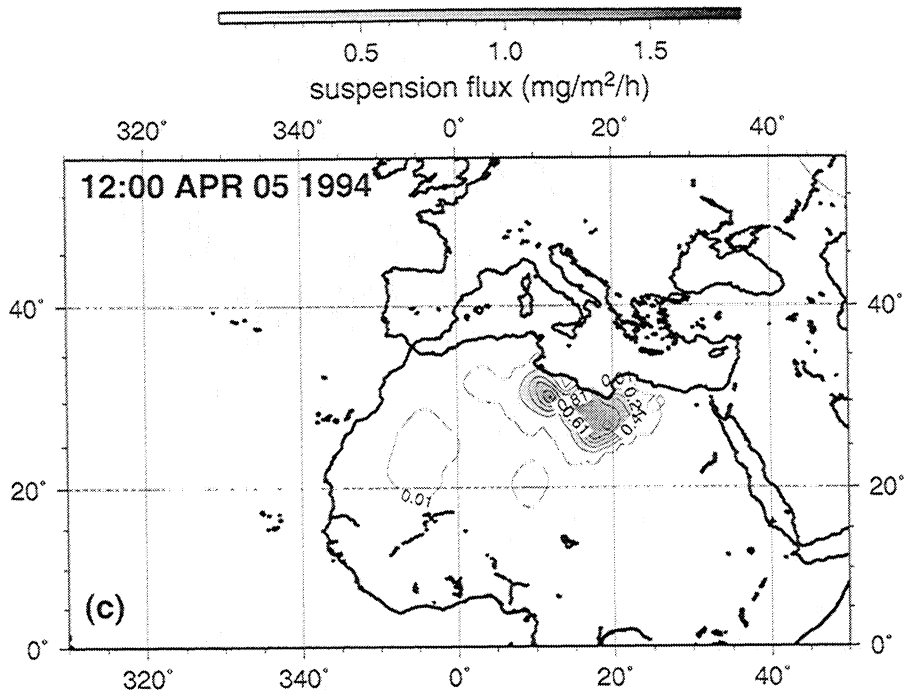

Figure 4. (continued)

studied by *Tegen and Fung* [1995], rather than the natural (desert) sources (Figure 1) included in our model study. This feature could be related to the "middle-level easterly jet" located near the southern boundary of the dust containing "Saharan Air Layer" moving west from Africa as described by *Karyampudi et al.*, [1999]. The easterly jet occurring near the frontal area of the dust plume after being lifted up into the "Saharan air layer" would indeed be consistent with the density contrast expected near the dust front.

There is striking correspondence between the observations and the model results concerning the crescent shaped patch of dust spreading into the Atlantic Ocean from sources in western Sahara (Figure 4a, Plate 1), and the dust patches over land as revealed by IDDI (Plates 1a-1e) and the model-generated source areas (Figures 4a-4c). The filament-like shape of the dust plume detached from northwest Africa and therefore appearing to be issuing from the sub-Saharan/Sahel region has been puzzling researchers in the past (see *Mbourou et al.* [1997] and *Husar et al.* [1997] for a discussion). The aerosol measurements based on the Nimbus 7/TOMS satellite data confirm that moderate to high dust concentrations occur most frequently in the western Sahara desert and in an area extending west into the subtropical Atlantic Ocean [*Herman et al.*, 1997]. Recent studies based on analysis of lidar data, have definitively shown the maximum values of AOD for the dust plume to be located in western Sahara, west of the Ahaggar massif in southern Algeria and, surprisingly, farther north over land than the latitude at which it apparently spreads into eastern Atlantic [*Karyampudi et al.*, 1999]. This is consistent with the above results.

Around April 15 a renewed cyclogenesis near the Atlas Mountains takes place, and on April 16 (Plate 1h), this cyclone once again moves north, transporting dust under the clouds. On April 17 the storm moves to the Balkans. Yellow rain was reported in Belgrade on the night of April 15-16, which was clearly associated with African cyclogenesis affecting the Balkans by *Vukmirovic et al.* [1997].

The model results show Sahara dust sources (increased surface fluxes) on April 3-5 (Figures 4a-4c) very similar to the areas indicated by IDDI over land in Plates 1a-1d. Increased surface fluxes are generated in regions of increased wind stress, and a result of the increased surface winds. The source, which is initially in the western Sahara on April 3 and 4 (Figures 4a, 4b) is related to the increased surface wind stress resulting from subsidence of air over Africa. A different source, namely resulting from the increased winds of the cyclone east of the Atlas Mountains starts to be active on April 4. On April 5 the first source region dies away, and the cyclonic center in the Gulf of Sirte becomes more active (Figure 4c). The friction velocity u_* generated by the model on April 4 (Figure 5) indicates that the surface shear stress is increased in the regions of increased fluxes (Figure 4b). A review of similar fields during a full daily cycle reveals that the surface stresses, and hence the fluxes of dust from the land surface to the atmosphere, increase during the less stable daytime boundary layer conditions and reach a peak in the afternoon hours.

Separate sources of dust activated by subsidence and cyclone-generated winds during April 3-6 create an exceptional pattern of dust transport, with one part of the

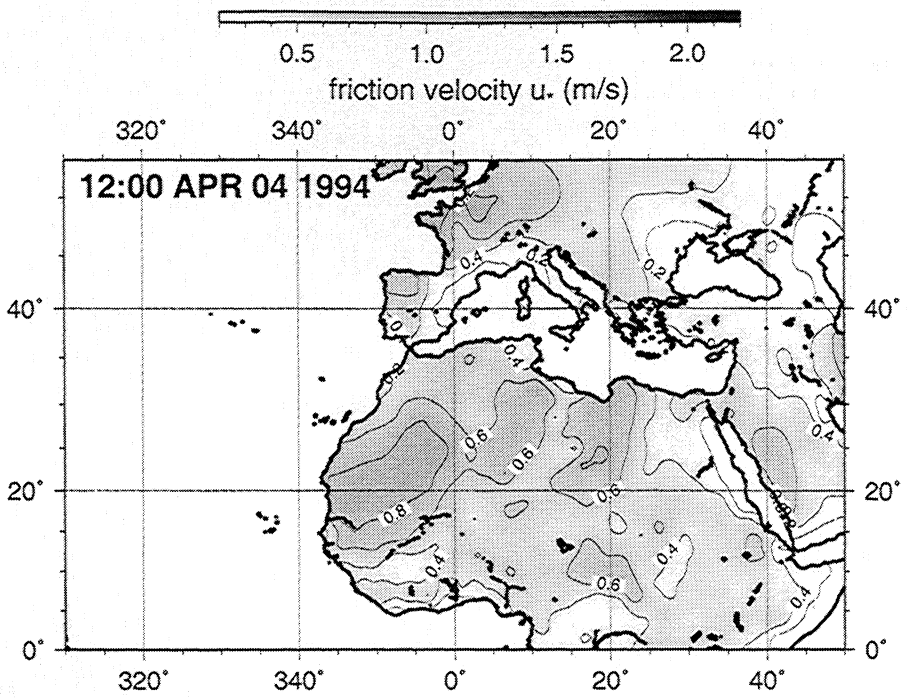

Figure 5. Model friction velocity $u_\star$ (m/s) on April 4, 1994, at 1200 UTC.

dust cloud moving across the Atlantic with the anticyclonic flow, and the other part transferred north toward the eastern Mediterranean and Balkans by a cyclonic depression. The dust spreads to the adjoining regions from a temporally changing source region. The model generated dust load on April 6 is shown in Figure 6a. While the combined Meteosat derived dust image on the same day in Plate 1d shows dust hidden under clouds of a cyclone in the eastern Mediterranean; the extent of dust is not clear because of poor resolution based on a

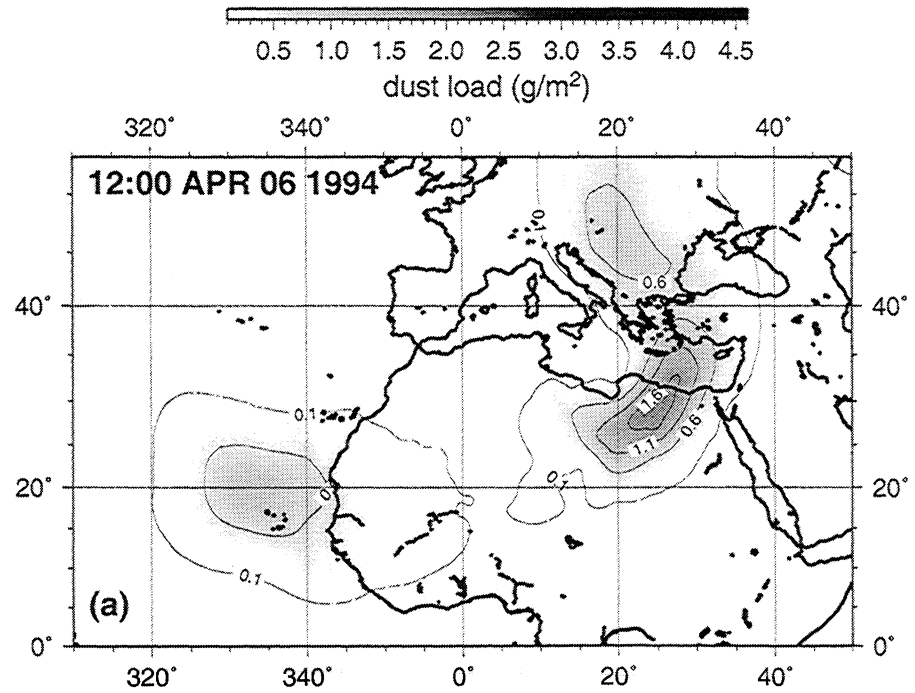

Figure 6. (a) Model dust load on April 6, 1200 UTC, (b) NOAA AVHRR image of dust storm on April 6, 1428 UTC and (c) light extinction coefficient derived from visibility observations on April 6, 1994.

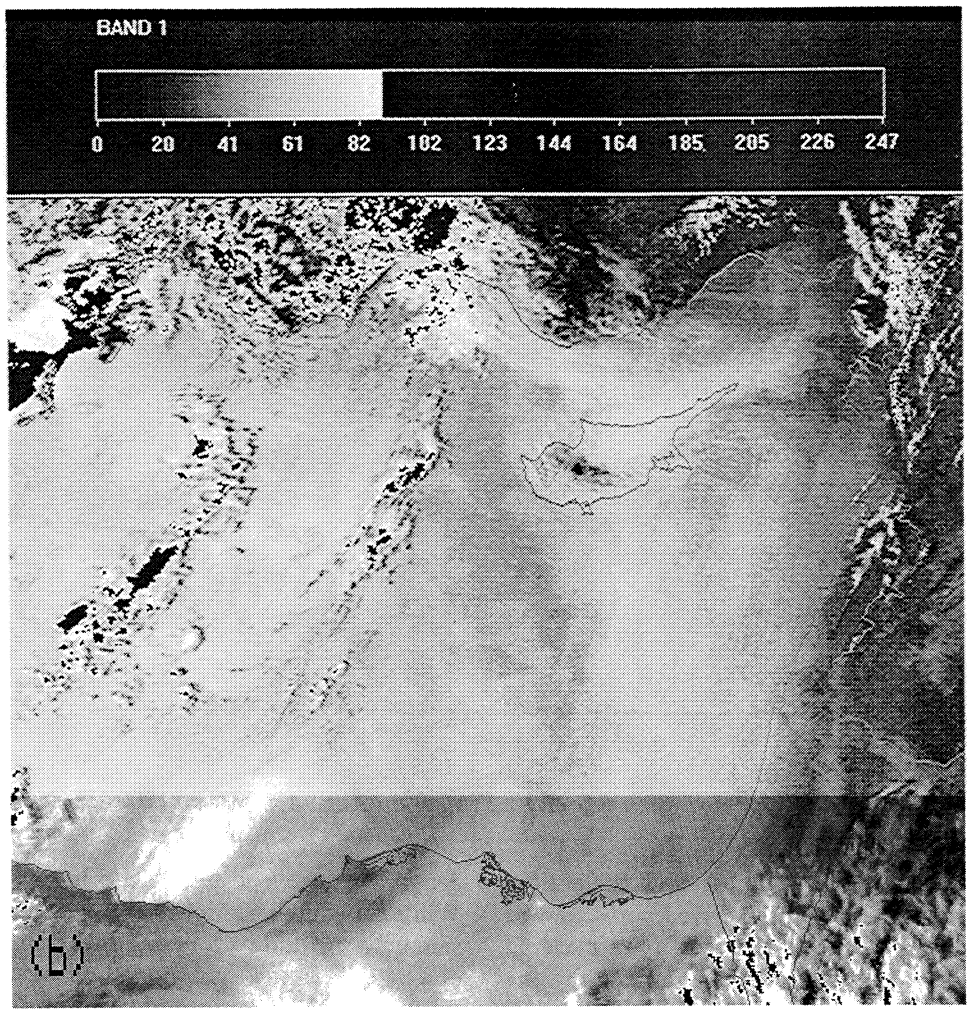

visibility / extinction (km^{-1}) 06 April 1994

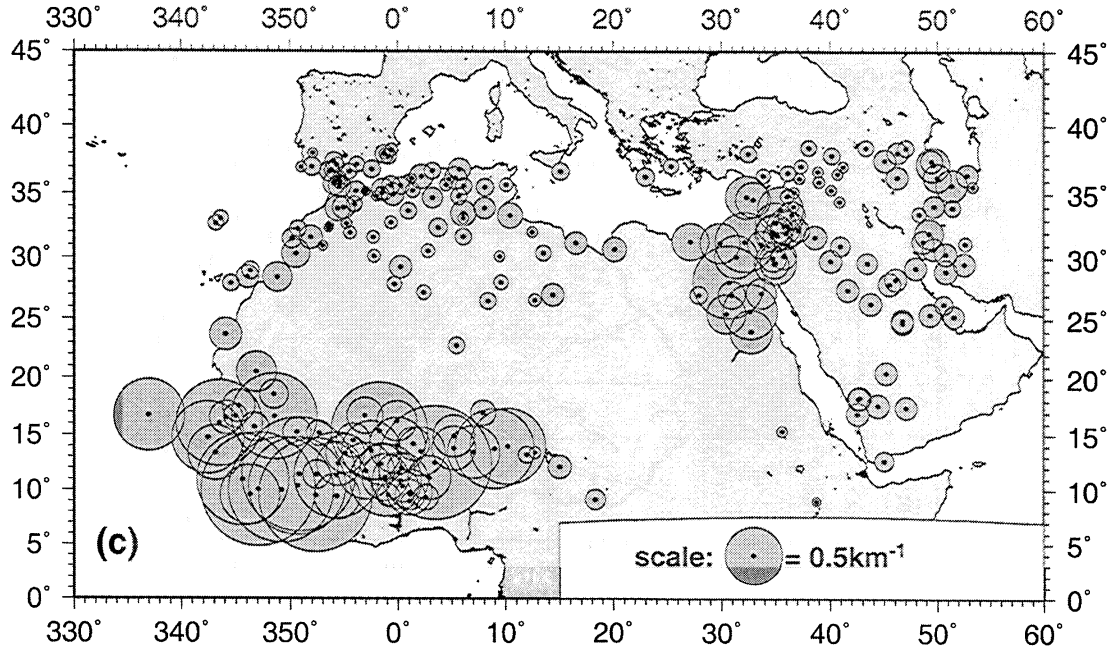

Figure 6. (continued)

nominal pixel size of 30 km. The NOAA AVHRR visible image (Figure 6b) with finer nominal resolution of about 1 km on the same day shows a better defined, shallow, dust cloud exiting from Egypt and being partially trapped by mountain ranges around the Levantine coast. The same cloud is observed to be partially overtopping the Anatolian topography to reach into the Black Sea (visible on larger area AVHRR coverage but not shown here). On the next day, AVHRR images and the model results show a marked decrease in the airborne dust (not shown) as a result of dry deposition. Although not directly comparable with dust load, further verification of increased dust concentration at the land surface, corresponding to patches moving into the Atlantic Ocean and the eastern Mediterranean Sea respectively, is provided by the distribution of extinction coefficient derived from visibility observations (Figure 6c). Both in the eastern part of the Levantine basin and along the Atlantic coasts of Africa, the extinction coefficient increases during the passage of the dust cloud.

The dust transport from Africa toward the Balkan peninsula, observed to occur for a second time on April 12-13 in Plates 1f and 1g, is reproduced by the model results in Figure 7a. Similarly, a later storm observed on April 15-16 in Plate 1h is shown to correspond to the model dust event in Figure 7b. During the latter event, wet dust deposition in the model takes place around northern Italy and Yugoslavia (Figure 7c) and was confirmed by ground measurements at Belgrade by *Vukmirovic et al.* [1997].

For revealing the three dimensional (3-D) structure of the combined dust storm on April 5, perspective views of the horizontal winds at 1.35 km altitude, the streamlines along a vertical cross section, and the dust isosurface 350 $\mu g/m^3$ are shown in Plate 2. The colors superimposed on the dust isosurface are propostional to vertical velocity on this surface, with red and blue corresponding to respective areas of upward and downward motion. The subsidence south of the Atlas Mountains on April 4 is evident in Plate 2, where the blue "dimple" on the dust isosurface shows downward motions resulting in the flattening of the isosurface by divergence. This is why the dust being transferred to the Atlantic Ocean has a very shallow structure, confined within the first few kilometers of the atmosphere, mainly transported above the intensified trade winds system. This structure of the trade winds, supplied by subsidence along the periphery of the North Atlantic anticyclone, is well known [*Tucker and Barry,* 1984]. On the other hand, in the eastern Mediterranean the dust put into motion by the Sirte cyclone penetrates upward along the warm front of the storm center by convection and frontal uplifting (Plate 2). A further feature noted in Plate 2 is the simultaneous dust storms generated near the Caspian and Aral Seas, in the far northeastern corner of the model domain, where increased near-surface winds mobilize dust from local deserts.

In the subtropical Atlantic the troposphere can generally be divided into a lower moist and an upper dry layer, the moist layer being capped by the trade wind

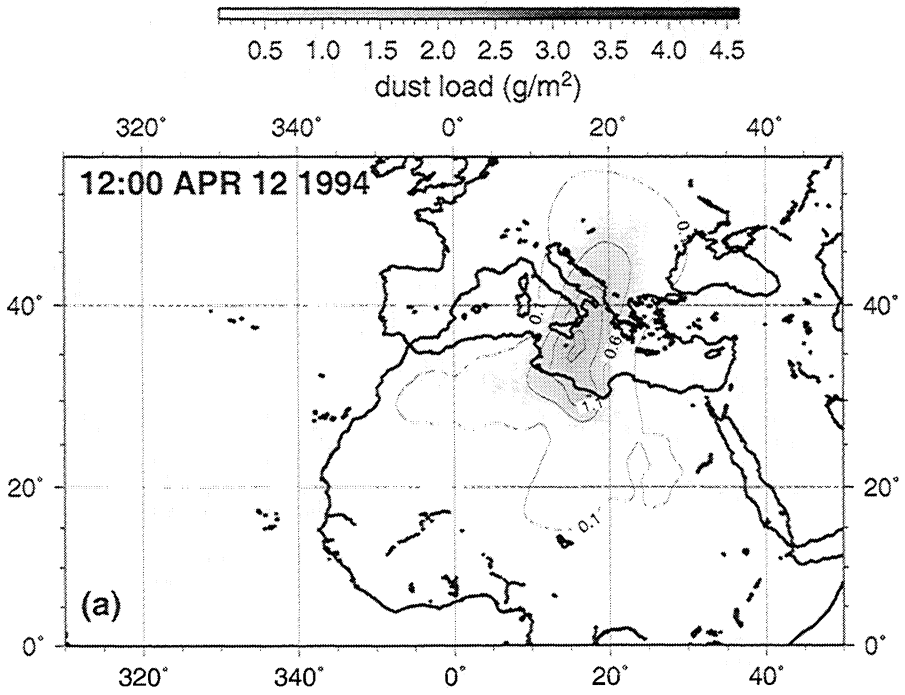

Figure 7. Model dust load on (a) April 12, 1200 UTC, (b) April 16, 1200 UTC, and (c) model wet dust deposition on April 17, 1994, 1200 UTC.

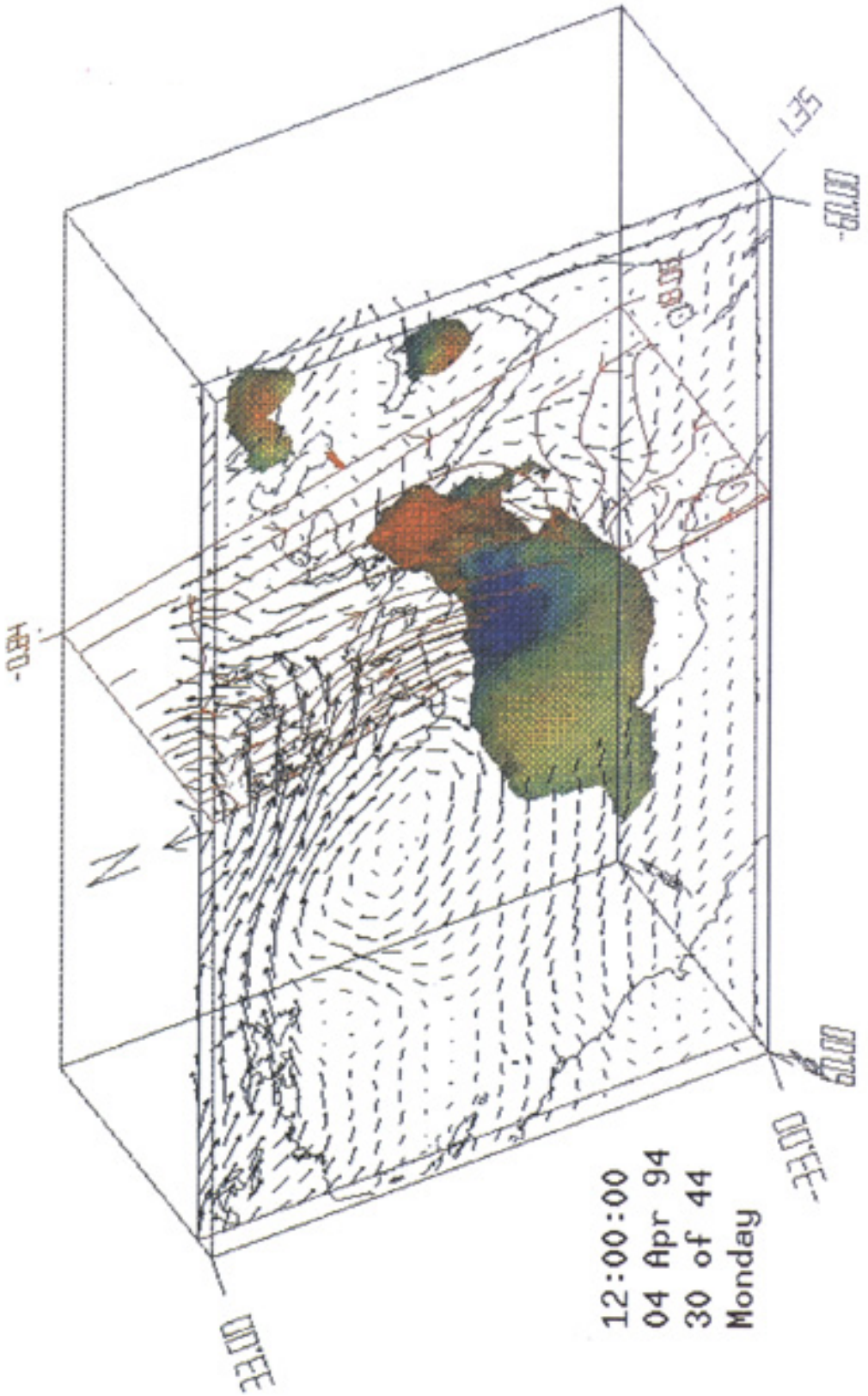

Plate 2. Three dimensional visualization of model results: horizontal wind at 1.35 km elevation, the streamlines on a vertical crosssection across Europe and Africa, dust isosurface for 350 $\mu g/m^3$, with coloring based on the same isosurface vertical velocity on April 5. Red/blue colors on the isosurface, respectively, correspond approximate levels of ± 0.02 m/s in vertical velocity.

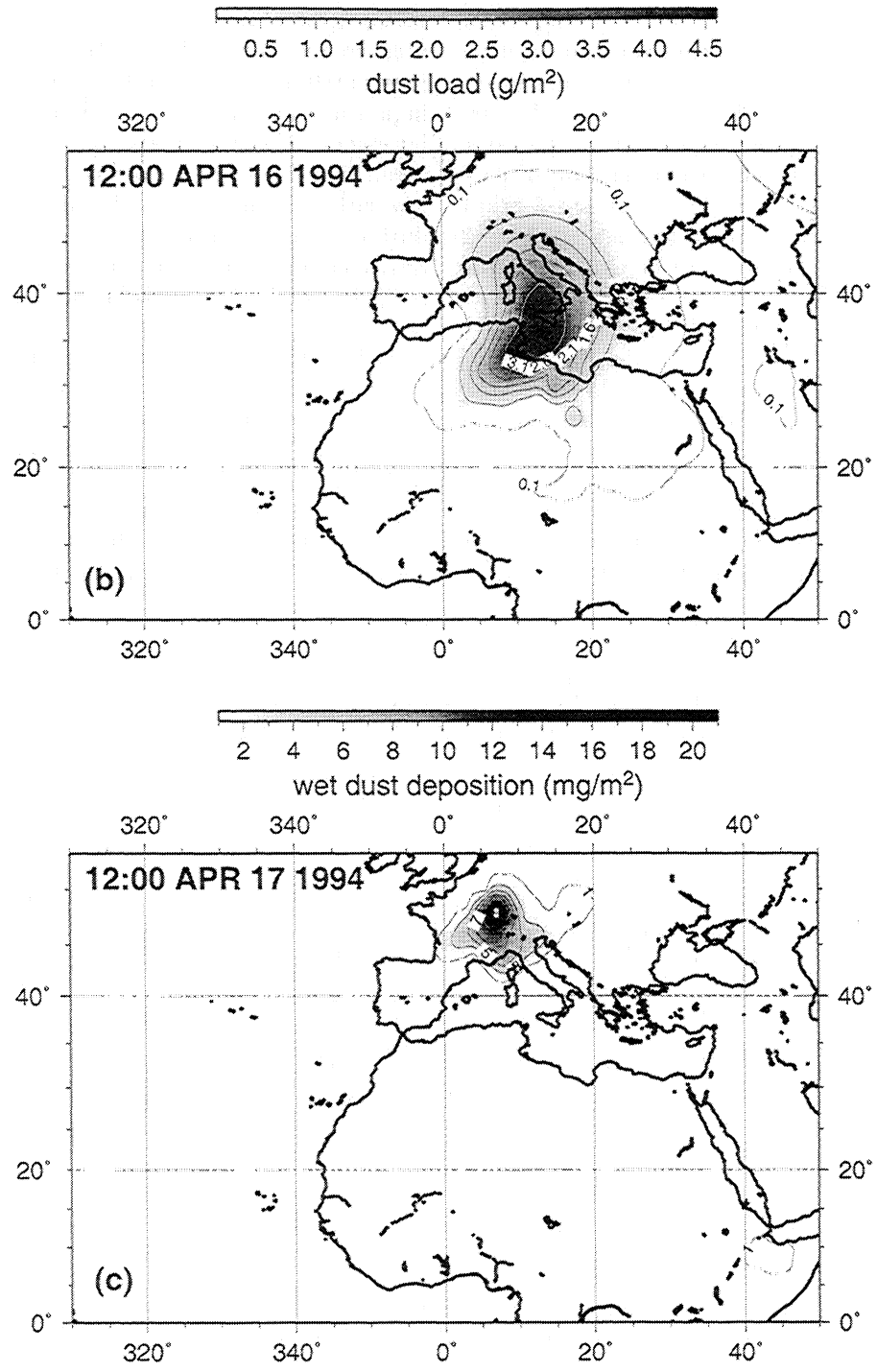

Figure 7. (continued)

inversion. The shallow trade wind inversion near the African coast (around 15°N) is strengthened by the effects of subsidence on the eastern side of the subtropical anticyclone and cooling from below by the cold upwelled water along the African coast [*Riehl,* 1954]. The temperature inversion in the eastern subtropical Atlantic does not coincide with the top of the trade wind regime, but is usually much shallower, at about an elevation of 500 m near Africa. The thickness of the moist surface layer depends on the balance of convection and subsidence, and sharply rises to 2-3 km in the west, characterized with trade wind cumuli formed near the Caribbean [*Byers,* 1959]. The actual structure of the marine boundary layer over a region of variable sea surface temperature can be much more complex than described above [*Bretherton et al.,* 1995; *Wang et al.,* 1999], displaying a splitting of the layer into 2 by an inversion that is much shallower than the main inversion, time dependence, and changes in clouds and layer fluxes.

The air and dew point temperature profiles on a tephigram at the Sal Island rawind sounding station are shown in Figure 8. The shallow trade wind inversion caps relatively cooler and humid air near the surface. Immediately above the inversion there is a layer with almost isentropic (potential temperature of 35°-45°C) and well mixed moisture (mixing ratio 1-2 g/kg) properties, most likely to be the air mass originating from the Sahara [*Karyampudi and Carlson,* 1988; *Chiapello et al.,* 1999]. Other rawinsonde data available at Dakar and Trinidad showed increasing temperature and humidity below the trade wind inversion, an increasing height of the surface mixed layer, and a decreasing thickness of the dust-containing layer above, from the African coast to the Caribbean region, as described by *Karyampudi et al,* [1999].

To exemplify the vertical structure of the trade wind system off western Africa, wind and dust concentration profiles obtained from the model at Sal Island on 1200 UTC, April 4, 1994, are shown in Figure 9. The wind veers to a northeasterly direction below the trade wind inversion from the generally easterly flow above it. The humid air mass is almost entirely trapped below the inversion. The dust maximum occurs at a height of about 500 m, in a layer immediately above the shallow surface layer. The model-simulated instantaneous dust concentrations are compared with the available dust concentration measurements and light extinction coefficient derived from visibility observations in Figure 10.

At Barbados Islands the model predictions were considerably lower than the measurements, although the timing of the peak period was not dramatically different. The maximum measured concentrations of 280 $\mu g/m^3$ represented an all-time high in the observation period of 30 years [*Li et al.,* 1997].

At Sal Island, the available measurements indicated dust concentrations reaching a peak of about 260 $\mu g/m^3$

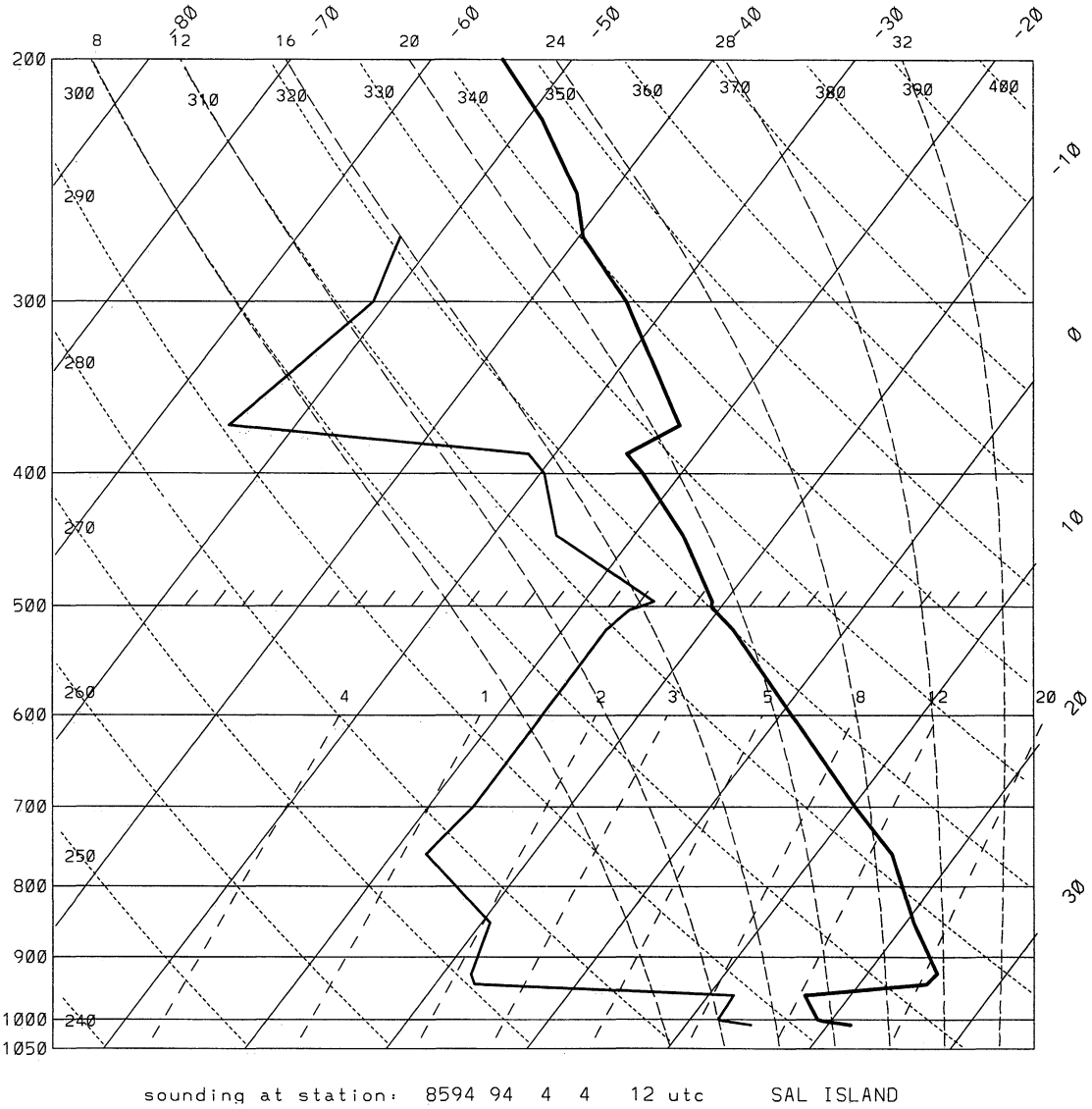

Figure 8. Tephigram from a rawindsonde profile at Sal Island on April 4, 1994, 1200 UTC.

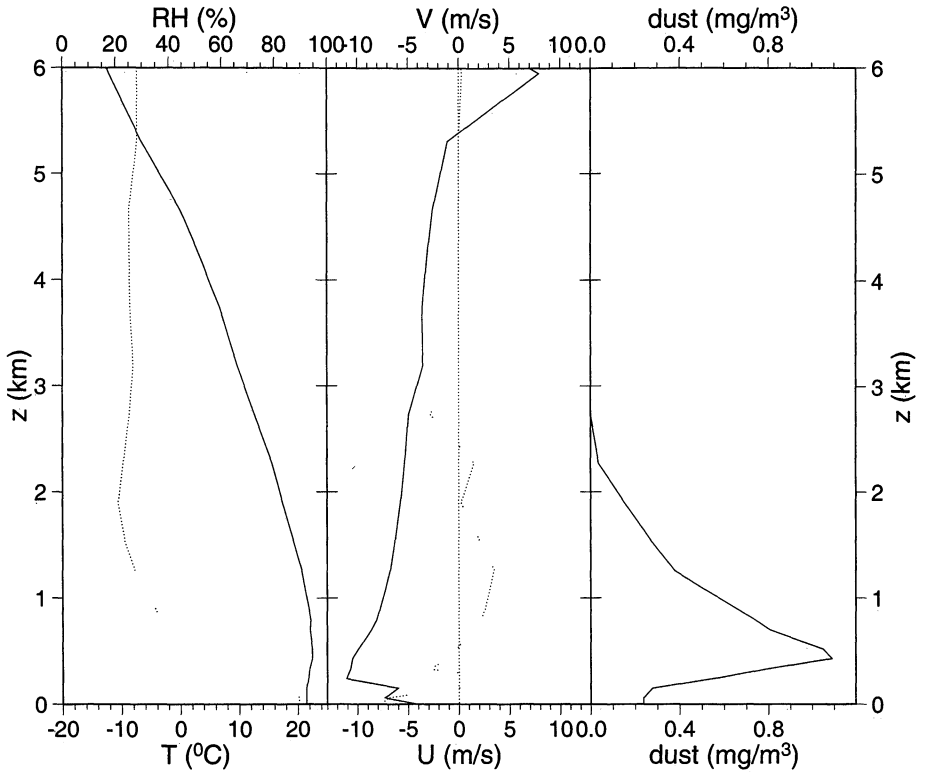

Figure 9. Vertical structure of the trade wind system obtained from the model: temperature, relative humidity (dotted line), east and north (dotted line) wind speed, and dust concentration profiles at Sal Island on April 4, 1994, 1200 UTC.

on April 5, which appeared approximately at the same time, but much smaller than the model-predicted maximum concentrations. Considering the shallow structure of dust close to the source region and the relatively poor resolution of the present model in the lower layers, this agreement is considered to be satisfactory. The measured peak concentrations in April 1994 are remarkably higher than the maxima observed in the months of April during the previous years of 1992 and 1993 [*Chiapello et al.*, 1995; 1997]. At the Erdemli station the observed peak concentration of 1600 $\mu g/m^3$ on the evening of April 6 and its decrease on April 7 agrees well with the model-calculated concentrations, and with the satellite observations of Figure 6.

To check if the model simulations produced similar results with the satellite observations, we compare the dust load at three selected locations in Figure 11. According to *Dulac et al.* [1992] the AOD derived from Meteosat can be converted to air column integrated dust load in g/m^2, by multiplying AOD with a calibration constant in the range of 1.3-1.5. We have used a factor of 1.4 and plotted model-derived and Meteosat-derived dust load together. The Mediterranean is mostly cloud covered, and therefore few Meteosat data points can be obtained at Erdemli to compare with the model results. In the Atlantic region the density front of the dust plume and the shallow transport are harder to simulate by the model. Despite these adverse factors the timing of dust pulses and order of magnitude agreement between satellite observations and model results are considered to be satisfactory.

3.3. Teleconnections and the North Atlantic Oscillation

The rather exceptional case of blocking and jet stream interactions concurrent with the extreme dust event in April 1994 calls for an investigation of its teleconnections, such as with the North Atlantic Oscillation (NAO), as proposed by *Moulin et al.* [1997]. The time series of the seasonal NAO index for the last two decades is shown in Figure 12, where the months of March and April 1994 are observed to have relatively high NAO index values of 2.3 and 3.6, respectively. The peak index values for the positive phase NAO anomaly in Figure 12 corresponds to one of the largest eight events in the last 20 years. The average sea level pressure pattern for the studied period indicated a dipole of low pressure near Iceland and high pressure near the Azores, typical of the large-scale circulation characterized by the positive phase of NAO.

It often appears paradoxical that monthly or seasonal statistics are used to describe quasi-steady state properties of the atmosphere and to investigate dynamic processes such as the NAO. The coarse statistics hides the short-term variability and therefore appears unrelated with the day-to-day variability of synoptic and p17i-bly extreme dynamic events within the period of averaging. For example, the anomalous atmospheric con-

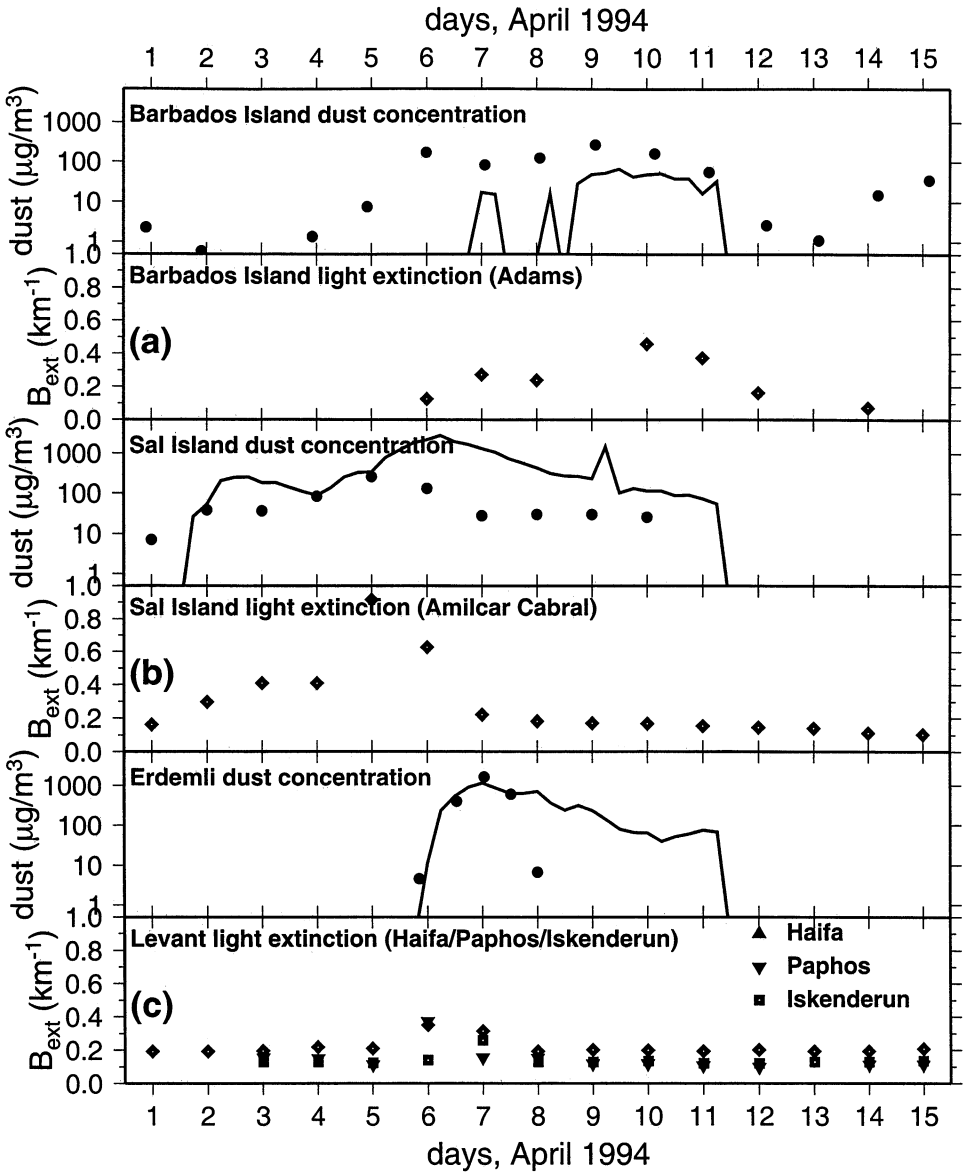

Figure 10. Comparison of model-simulated (lines) dust concentration time series with the available ground observations (points) and light extinction coefficient derived from visibility observations: Barbados, Sal Island, and Erdemli. (For light extinction in Erdemli, the data available at the closest stations Haifa, Paphos, and İskenderun have been plotted.)

ditions studied above are almost undetectable in the annual NAO index for 1994. This is despite the reliable correlation of dust and NAO on an annual basis [*Moulin et al.,* 1997], and the exceptional levels of dust concentration measured at Barbados [*Li, et al.,* 1996] and Erdemli corresponding to extreme blocking conditions (Figures 2 and 3) typical of NAO. It is not surprising to find poor statistical correlation between transport and large-scale circulation based on long-term averages. Seen from this point of view, large-scale atmospheric control is not readily inferred from coarse statistics unless studied carefully at the relevant time-scales.

4. Conclusions

We have demonstrated a genuine Mediterranean case of meridional circulation and jet interaction resulting from Atlantic blocking, an extreme event that produced the massive cloud of Sahara dust in April 1994. The interaction of the two jets, shown here, has been suggested (e.g., [*Reiter,* 1975] but, at least to the authors' knowledge, not adequately demonstrated as a principal mechanism of Mediterranean cyclogenesis, although some limited examples have been provided by *Karein,* [1979]. The Mediterranean/North African region is con-

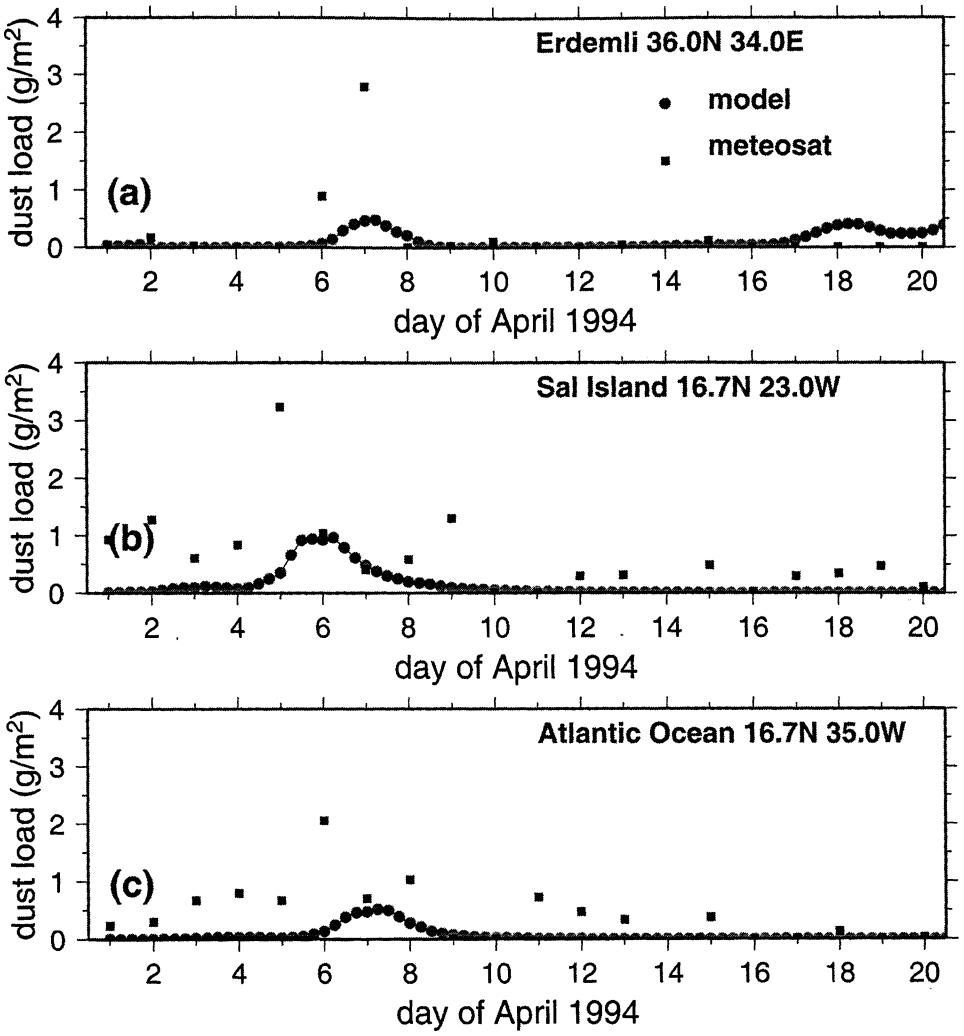

Figure 11. Model-derived (grey circles) versus Meteosat-AOD-derived (black squares) air column-integrated dust load (g/m^2) at (a) Erdemli, (b) Sal Island, and (c) a location in the Atlantic Ocean west of Sal Island. The Meteosat-derived AOD is converted to dust load as described in the text

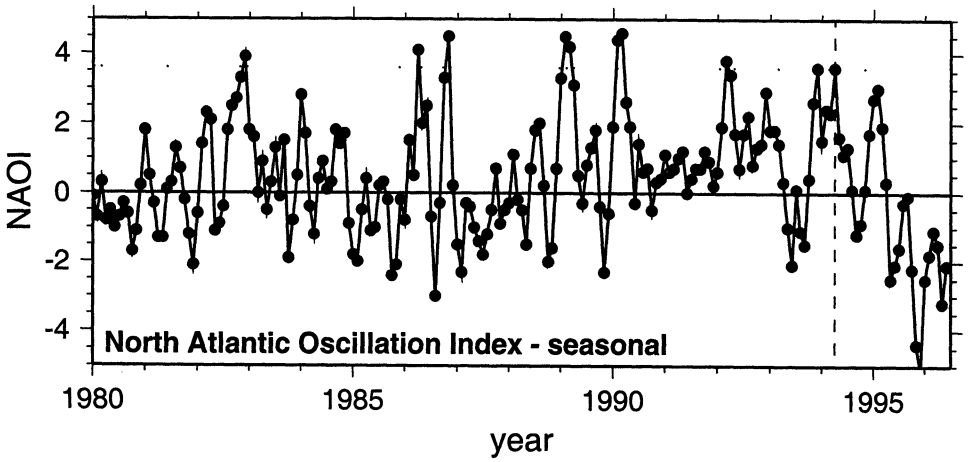

Figure 12. Time variation of the seasonal NAO index for the last two decades. The vertical dashed line is positioned at April 1994. The horizontal dotted line marks the NAOI value of 3.6 for the same month

sidered as one of the three global areas where active cyclogenesis could be driven by jet interactions, the first two relatively stronger centers being downstream of the Rocky and Himalaya mountain ranges, where the two jet streams, typically represented by a three-wave global pattern, come into contact [*Reiter,* 1975, *Özsoy,* 1981]. In the case of the Mediterranean, meridional flow and jet interactions are expected east of a blocking high-pressure system in the Atlantic, occasionally taking the form of an "omega high" near Spain. This type of circulation often characterizes northwesterly mistral winds across the gap between the Pyrenees and the Alps, in some cases associated with Genoa cyclogenesis, and largely influencing the western and south central Mediterranean with cold, dry air resulting from subsidence [*Reiter,* 1975; *Brody and Nestor,* 1980].

The maximum concentration of dust measured in April 1994 at the Barbados island represented an extreme event possibly carrying the signatures of a large-amplitude climatic fluctuation. We emphasize the role of large-scale atmospheric control in creating the dust event and show that the sequence of events leading from a strong case of atmospheric blocking, to undulations of the polar jet, its interactions and exchange of mass and energy with the subtropical jet, cyclogenesis driven by barotropic/baroclinic instabilities, subsidence and strengthening of trade winds, etc., make up the ingredients of the studied dust transport event. We also find that this kind of hemispherical weather is associated with a prominent example for the NAO transient and hence strengthen the earlier attempts to correlate dust transport with characteristic teleconnection patterns; however, we do that on an event basis, rather than using statistical analyses on annual to seasonal time-scales as considered in earlier literature.

One of the successes of our model simulations is the long-range transport of dust. Simulated dust conditions at sites distant from the source regions agree well with the observations, even under adverse conditions of subsidence and shallow boundary layer structures present in the Atlantic region. Available ground measurements and satellite data confirm the modeling results and analyses in a large area of the hemisphere. The incursion of the jet circulation into Africa creates surface suspensions of dust propagating simultaneously but in two different directions into the Atlantic and Mediterranean regions. The two pulses are dissimilar in their characteristics, representing different meteorological conditions, and mesoscale characteristics; yet they are successfully simulated by the model, with an order of magnitude agreement between model results and observations. Dust reaching the Barbados islands is underestimated, as a result of specific planetary boundary layer processes of the trade wind and the trade inversion regimes not fully resolved and inadequately calibrated in the present model. These results also imply that an appropriate representation of dust size classification would be required in the model for better simulation of the long-range transport.

Acknowledgments. Modeling was performed at the Institute of Marine Sciences of the Middle East Technical University (IMS-METU) with support from the NATO TU-REMOSENS Project, thanks to Cemal Saydam of METU. AVHRR satellite data for dust events were collected at the the IMS-METU, with support from the NATO SfS project 'TU-Black Sea' and the NATO SfP project 'ODBMS Black Sea'. Measurements of dust at Erdemli were obtained within research projects of the Turkish Scientific and Technical Research Council (TÜBİTAK) project DEBAG-79/G and METU Research Fund project AFP-98-06-01-01. Another TÜBİTAK project YDABÇAG-615/G motivated and helped production of this paper. Barbados dust measurements obtained as a part of the AEROCE program kindly have been supplied by Joe Prospero (University of Miami). Ground truth measurements at Sal Island were supplied by L. Gomes of the Université de Paris, France. Extinction coefficients retrieved from WMO visibility measurements were provided by J. Husar and R. Husar, Center for Air Pollution and Trend Analysis, Washington University.

References

Alpert, P., and E. Ganor, A jet-stream-associated heavy dust storm in the western Mediterranean, *J. Geophys. Res., 98,* 7339-7349, 1993.

Alpert, P., and B. Ziv, The Sharav cyclone: Observations and some theoretical considerations, *J. Geophys. Res., 94,* 18495-18515, 1989.

Alpert, P., Y. J. Kaufman, Y. Shay-El, D. Tanre, A. da Silva, S. Schubert, and J. H. Joseph, Quantification of dust-forced heating of the lower troposphere, *Nature, 395,* 367-370, 1998.

Andreae, M. O., Raising dust in the greenhouse, *Nature, 380,* 389-390, 1996.

Avila, A. and J. Peñuelas, Increasing frequency of Saharan rains over northeastern Spain and its ecological consequences, *Sci. Total Environ., 228,* 153-156, 1999.

Bretherton, C. S., P. Austin, and D. T. Siems, Cloudiness and marine boundary layer dynamics in the ASTEX Lagrangian Experiments, part II, Cloudiness, drizzle, surface fluxes, and entrainment, *J. Atmos. Sci., 52,* 2724-2735, 1995.

Brody, L. R., and M. J. R. Nestor, Regional forecasting aids for the Mediterranean basin, Handbook for Forecasters in the Mediterranean, part 2, *Tech. Rep. TR 80-10,* 178 pp., Naval Environ. Predict. Res. Facil., Monterey, Calif., 1980.

Byers, H. R., *General Meteorology,* McGraw-Hill, New York, 1959.

Chamberlain, A. C., Roughness length of sea, sand and snow. *Boundary Layer Meteorol., 25,* 405-409, 1986.

Chiapello, I., G. Bergametti, L. Gomes, B. Chatenet, F. Dulac, J. Pimenta, and E. Santos Suares, An additional low layer transport of Sahelian and Saharan dust over the northeastern tropical Atlantic, *Geophys. Res. Lett., 22,* 3191-3194, 1995.

Chiapello I., G. Bergametti, B. Chatenet, P. Bousquet, F. Dulac, and E. Santos Soares, Origins of African dust transported over the northeastern tropical Atlantic, *J. Geophys. Res., 102,* 13,701-13,709, 1997.

Chiapello I., G. Bergametti, B. Chatenet, F. Dulac, I. Jankowiak, C. Liousse, and E. Santos Soares, Contribution of the different aerosol species to the aerosol mass

load and optical depth over the northeastern tropical Atlantic, *J. Geophys. Res., 104,* 4025-4035, 1999.

Danielsen, E. F., The relationship between severe weather, major dust storms and rapid cyclogenesis, in *Synoptic Extratropical Weather Systems*, edited by M. Shapiro, pp. 215-241, Nat. Cent. for Atmos. Res., Boulder, Colo., 1974.

Dentener, F. J., G. R. Carmichael, Y. Zhang, J. Lelieveld and P. J. Crutzen, Role of mineral aerosol as a reactive surface in the global troposphere, *J. Geophys. Res., 101,* 22,869-22,889, 1996.

Duce, *et al.*, The atmospheric input of trace species to the world ocean, *Global Biogeochem. Cycles, 5,* 193-256, 1991.

Dulac, F., D. Tanre, G. Bergametti, P. Buat-Menard, M. Desbois and D. Sutton, Assessment of the African airborne dust mass over the Mediterranean Sea using Meteosat data, *J. Geophys. Res., 97,* 2489-2506, 1992.

Egger, J., P. Alpert, A. Tafferner, and B. Ziv, Numerical experiments on the genesis of Sharav cyclones: Idealized simulations, *Tellus, Ser. A, 47,* 162-174, 1995.

El-Tantawy, A. E.-H. I., The role of the jet stream in the formation of desert depressions in the Middle East, *WMO Tech. Note 64*, pp. 159-171, World Meteorol. Organ., Geneva, Switzerland, 1961.

Flierl, G. R., V. D. Larichev, J. C. McWilliams, and G. Reznik, The dynamics of baroclinic and barotropic solitary eddies, *Dyn. Atmos. Oceans, 5,* 1-41, 1980.

Gilman, C., and C. Garrett, Heat flux parameterizations for the Mediterranean Sea: The role of atmospheric aerosols and constraints from the water budget, *J. Geophys. Res., 99,* 5119-5134, 1994.

Guerzoni, et al., The role of atmospheric deposition in the biogeochemistry of the Mediterranean Sea, *Prog. Oceanogr., 44*, 147-190, 1999.

Herman, J. R., P. K. Bhartia, O. Torres, C. Hsu, C. Seftor, and E. Celarier, Global distribution of UV-absorbing aerosols from Nimbus 7/TOMS data, *J. Geophys. Res., 102,* 16,911-16,922, 1997.

Husar, R. B., and J. D. Husar, Global Distribution of Continental Haziness, Web URL: http://capita.wustl.edu/CAPITA/CapitaReports/GLOBVIZ/GLOBVIS1.html, 1998.

Husar R. B., J. M. Prospero, and L. L. Stowe, Characterization of tropospheric aerosols over the oceans with the NOAA advanced very high resolution radiometer optical thickness operational product, *J. Geophys. Res., 102,* 16,889-16,909, 1997.

Janjic, Z.I., Pressure gradient force and advection scheme used for forecasting with steep and small scale topography, *Contrib. Atmos. Phys., 50*, 186-199, 1977.

Janjic, Z. I., Non-linear advection schemes and energy cascade on semi-staggered grids, *Mon. Weather Rev., 112,* 1234-1245, 1984.

Janjic, Z. I., The step-mountain coordinate: Physical package, *Mon. Weather Rev., 118,* 1429-1443, 1990.

Janjic, Z. I., The step-mountain Eta Coordinate Model: Further developments of the convection, viscous sublayer and turbulence closure schemes, *Mon. Weather Rev., 122,* 927-945, 1994.

Karein, A. A., The forecasting of cyclogenesis in the Mediterranean region, Ph.D. thesis, 159 pp., Univ. of Edinburgh, Edinburgh, Scotland, 1979.

Karyampudi, V. M. and T. N. Carlson, Analysis and numerical simulations of the Saharan air layer and its effect on easterly wave disturbances, *J. Atmos. Sci., 45,* 3102-3136, 1988.

Karyampudi, M. V., et al., Validation of the Saharan dust plume conceptual model using Lidar, Meteosat, and ECMWF data, *Bull. Am. Meteorol. Soc., 80,* 1045-1076, 1999.

Kubilay, N., and A. C. Saydam, Trace elements in atmospheric particulates over the eastern Mediterranean; Concentrations, sources, and temporal variability, *Atmos. Environ., 29,* 2289-2300, 1995.

Kubilay, N., S. Nickovic, C. Moulin, and F. Dulac, An illustration of the transport and deposition of mineral dust onto the eastern Mediterranean, *Atmos. Environ., 34,* 1293-1303, 2000.

Li, X., H. Maring, D. Savoie, K. Voss, and J. M. Prospero, Dominance of mineral dust in aerosol light scattering in the North Atlantic trade winds, *Nature, 380,* 416-419, 1996.

Mbourou, G. N., J. J. Bertrand and S. E. Nicholson, The diurnal and seasonal cycles of wind-borne dust over Africa north of the Equator, *J. Appl. Meteorol., 36,* 868-882, 1997.

McWilliams, J. C., An application of equivalent modons to atmospheric blocking, *Dyn. Atmos. Oceans, 5,* 43-66, 1980.

Mesinger, F., Z. I. Janjic, S. Nickovic, D. Gavrilov, and D. G. Deaven, The step-mountain coordinate: model description and performance for cases of Alpine lee cyclogenesis and for a case of an Appalachian redevelopment, *Mon. Weather Rev., 116,* 1493-1518, 1988.

Miller, R. L., and I. Tegen, Climate response to soil dust aerosols, *J. Clim., 11,* 3247-3267, 1998.

Miller, R. L., and I. Tegen, Radiative forcing of a tropical direct circulation by soil dust aerosols, *J. Atmos. Sci., 56,* 2403-2433, 1999.

Moulin, C., C. E. Lambert, F. Dulac, and U. Dayan, Control of atmospheric export of dust from North Africa by the North Atlantic oscillation, *Nature, 387,* 691-694, 1997.

Moulin, M. C., Transport atmospherique des poussieres africaines sur la Mediterranée et l'Atlantique: Climatologie satellitale a partir des images Meteosat VIS (1983-1994) et relations avec le climat, Ph.D. Thesis, Univ. Paris, France, 1997.

Nickovic, S., and S. Dobricic, A model for long-range transport of desert dust, *Mon. Weather Rev., 124,* 2537-2544, 1996.

Nickovic, S., D. Jovic, O. Kakaliagou, and G. Kallos, Production and long-range transport of desert dust in the Mediterranean region: Eta model simulations, paper presented at the 22nd International Technical Meeting on Air Pollution Modelling and Its Applications, NATO/CCMS, 2-6 June 1997, Clermont-Ferrand, France, 1997.

Nickovic, S., G. Kallos, A. Papadopoulos, and O. Kakaliagou, A model for prediction of desert dust cycle in the atmosphere, *J. Geophys. Res.*, this issue.

Ott, S. T., A. Ott, D. W. Martin, and J. A. Young, Analysis of a trans-Atlantic Saharan dust outbreak based on satellite and GATE data, *Mon. Weather Rev., 119,* 1832-1850, 1991.

Özsoy, E., On the atmospheric factors affecting the Levantine Sea, *Tech. Rep. 25,* 30 pp., Eur. Cent. for Medium-Range Weather Forecasts (ECMWF), Reading, England, 1981.

Özsoy, E., Sensitivity to global change in temperate Euro-Asian seas (the Mediterranean, Black Sea and Caspian Sea): A review, in *The Eastern Mediterranean as a Laboratory Basin for the Assessment of Contrasting Ecosystems*, vol. 51, *Environmental Security, NATO Sci. Ser.,* vol. 2, edited by P. Malanotte-Rizzoli and V. N. Eremeev, pp. 281-300, Kluwer Acad., Norwell, Mass., 1999.

Perry, K. D., T. A. Cahill, R. A. Eldred, and D. D. Dutcher, Long-range transport of North-African dust to the east-

ern United States, *J. Geophys. Res., 102*, 11,225-11,238, 1997.

Prezerakos, N. G., Synoptic flow patterns leading to the generation of north-west African depressions, *Int. J. Climatol., 10,* 33-48, 1990.

Prezerakos, N. G., Dust storms over Sahara desert leading to dust deposit or coloured rain in the south Balkans, in *First LAS/WMO International Symposium on Sand and Dust Storms (ISSDS-I), WMO/TD-864*, pp. 21-38, World Meteorol. Organ., Geneva, Switzerland, 1998.

Prezerakos, N. G., S. C. Michaelides, and A. S. Vlassi, Atmospheric synoptic conditions associated with the initiation of north-west African depressions, *Int. J. Climatol., 10,* 711-729, 1990.

Prospero, J. M., Arid regions as sources of mineral aerosols in the marine atmosphere, *Geol. Soc. Am., Spec. Pap. 186,* 71-86, 1981.

Prospero, J. M., and R. T. Nees, Impact of the north African drought and El Niño on mineral dust in the Barbados trade winds, *Nature, 320,* 735-738, 1986.

Reiter, E. R., Handbook for forecasters in the Mediterranean: Weather phenomena of the Mediterranean basin, part 1, General description of the meteorological processes, *Tech. Pap. 5-75,* 344 pp., Environ. Predict. Res. Facil., Nav. Postgrad. Sch., Monterey, Calif., 1975.

Riehl, H., *Tropical Meteorology,* 392 pp., McGraw-Hill, New York, 1954.

Schollaert, S. E. and J. T. Merrill, Cooler sea surface west of the Sahara desert correlated to dust events, *Geophys. Res. Lett., 25,* 3529-3532, 1998.

Science and Technology Corporation (STC), Asian dust-storms and their effects on radiation and climate, Part I, *Tech. Rep. 2906*, STC, Hampton, Va., 1995.

Science and Technology Corporation (STC), Asian dust-storms and their effects on radiation and climate, Part II, *Tech. Rep. 2959*, STC, Hampton, Va., 1996.

Segal, M., On the impact of thermal stability on some rough flow effects over mobile surfaces, *Boundary Layer Meteorol., 52,* 193-198, 1990.

Tegen, I., and I. Fung, Contribution to the atmospheric mineral aerosol load from land surface modification, *J. Geophys. Res., 100,* 18,707-18,726, 1995.

Tegen, I., A. A. Lacis, and I. Fung, The influence on climate forcing of mineral aerosols from disturbed soils, *Nature 380,* 419-422, 1996.

Tucker, G. B.. and R. G. Barry, Climate of the North Atlantic Ocean, in *Climates of the Oceans,* vol. 15, *World Survey of Climatology,* edited by H. Van Loon, pp. 193-257, Elsevier Sci., New York, 1984.

Vukmirovic, Z., J. Marendic-Miljkovic, S. Rajsic, M. Tasic, and V. Novakovic, Resuspension of trace metals in Belgrade under conditions of drastically reduced emission levels, *Water Air and Soil Pollut., 93*, 137-156, 1997.

Wallace, J. M. and M. L. Blackmon, Observations of low-frequency atmospheric variability, in *Large-Scale Dynamical Processes in the Atmosphere,* edited by B. J. Hoskins and R. P. Pearce, pp. 54-95, Academic, San Diego, Calif., 1983.

Wang, Q., et al., Characteristics of marine boundary layers during Lagrangian measurement periods, 1, General conditions and characteristics, *J. Geophys. Res., 104,* 21,751-21,765, 1999.

Wilson, M. F., and A. Henderson-Sellers, Land cover and soils data sets for use in general circulation climate models, *J. Climatol., 5,* 119-143, 1984.

N. Kubilay and E. Özsoy, Institute of Marine Sciences, Middle East Technical University P.K. 28 Erdemli, İçel 33731 Turkey. (kubilay@ims.metu.edu.tr); (ozsoy@ims.metu.edu.tr)

C. Moulin, Laboratoire des Sciences du Climat et de l'Environnement (CEA/CNRS), CE Saclay - bat.709, 91191 Gif-sur-Yvette, France. (moulin@lsce. saclay.cea.fr)

S. Nickovic, Euro-Mediterranean Centre on Insular Coastal Dynamics, Foundation for International Studies, University of Malta, St. Paul Street, Valletta, Malta. (nicko@icod.org.mt)

(Received August 29, 2000; revised November 27, 2000; accepted December 1, 2000.)